International Journal of Technical Innovation in Modern Engineering & Science (IJTIMES)
Impact Factor: 5.22 (SJIF-2017), e-ISSN: 2455-2585
Volume 4, Issue 07, July-2018

# Provenance signatures from whole rock Geochemistry of Archaean Metapelites from Eastern Dharwar Craton, Southern India.

Dr. N. Mahesha
*Assistant Professor, Department of Civil Engineering, NHCE-Bangalore, India,* `maheshangowda1982@gmail.com`

**Abstract**— ***In this paper an attempt has been made to present the major, trace and REE geochemistry, whole rock Sm-Nd and Rb-Sr isotope data of metapelites from different localities (Pavagada, Bidaloti, Bandihalli and Duntur) in the Eastern Dharwar Craton, in order to characterize the nature of provenance, weathering conditions, tectonic settings and crustal evolution. Major elements, trace element contents, Rb/Sr, Th/U, Zr/Y, Th/Sc, Nb/Ta, Zr/Hf, Cr/Ni, Ni/Co, Cr/Y, Eu/Eu* ratios and REE patterns of the studied metapelites indicate their derivation from provenance comprising varying proportions of ultramafic-mafic-intermediate source. Highly variable CIA and CIW values with low contents of Ca and Na indicate variable and locally moderate to intense weathering of the source rocks. On La/Sc Vs Ti/Zr, Co -Th-Zr/10, Sc-Th-Zr/10 and Th-La-Sc discriminating plots, the studied metapelites plot within the oceanic island arc and continental island arc fields, confirming the Arc provenance for the studied metapelites. The studied metapelites defines negative εNd values at 3000 Ma with $T_{DM}$ Nd model ages ranging from 3400 to 3600 Ma implies that their sources were derived from exotic sources localized outside the Dharwar craton (Today exposed terrains in western Australia, southern Africa or Antarctica) as all those fragments were once part of a supercontinent.***

***Keywords***— ***Metapelites, Eastern Dharwar Craton, Geochemistry, Provenance, Island arc, Supercontinent***

## I. INTRODUCTION

In Dharwar craton both low grade greenstone and as well as high grade terrains are well exposed. However, most of the studies focused on sediments of Archaean greenstone belts and Proterozoic basins (Manikyamba et al., 1993; 1997; Arora and Naqvi, 1993; Arora et al., 1994; Sambashiva Rao et al., 1999; Bhaskar Rao et al., 1995). However a few studies so far carried out on the sediments of high-grade terrain (Naqvi et al., 1983; Devaraju and Sadashivaiah, 1969; Anantha Iyer and Vasudev, 1976; Devaraju and Laajoki, 1986; Janardhan et al., 1986; 1990; Harris and Jayaram, 1982; Mahabaleswar et al., 1986; Appel and Mahabaleswar 1988; Mahabaleswar et al., 1989, 1995, 1995a; Kato et al., 1996), were aimed at characterizing the probable source of these sediments and P-T conditions of metamorphism as they contain mineral pairs suitable for these estimations. Not much attention was given on the sedimentary environments, nature and composition of contributing sources and thermal evolution. So it is proposed to study the well exposed high grade metapelites in Pavagada, Bidaloti, Bandihalli and Duntur areas (Fig. 1) of the Eastern Dharwar craton in order to address the nature of provenance, weathering conditions, tectonic settings and crustal evolution.

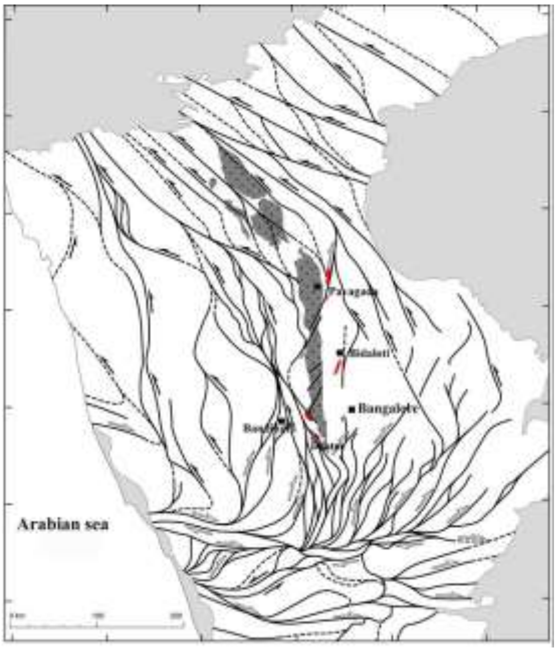

Fig. 1. Bird eye view of the studied areas bordering around Closepet granite (after Chardon et al 2008).

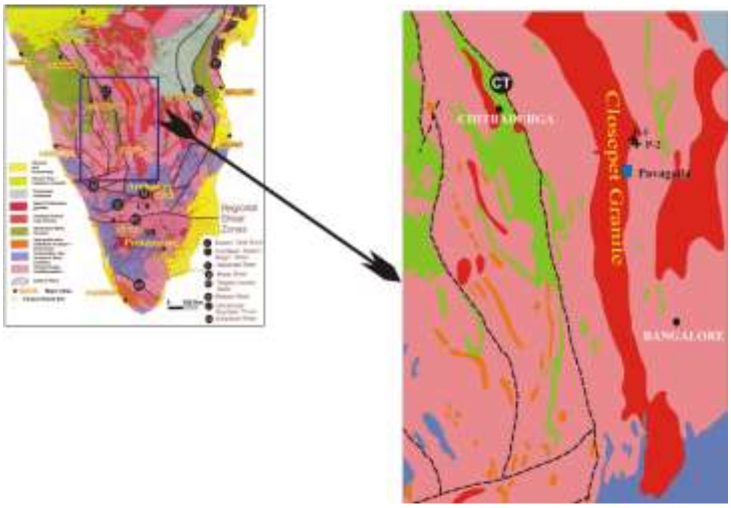

Fig. 2. Geological map of part of the Dharwar craton showing sample locations of Pavagada metapelites (after GSI Map).

## II. GEOLOGICAL SETTINGS

The exposed Archaean crust in the Eastern Dharwar Craton (EDC) comprises 2.7 - 2.6 Ga TTG-greenstone associations with minor remnants of >3.0 Ga basement enclaves (TTG and interlayered high grade supracrustal rocks) and most voluminous late 2.56 - 2.52 Ga calc-alkaline to potassic composite plutons (Krogstad et al., 1991; Friend and Nutman, 1992; Nutman et al., 1996; Peucat et al., 1993; Chardon et al., 2002). The most remarkable of these composite plutons is the 2.52 Ga old 400 km long and about 20 km wide N-S trending Closepet granite (Jayananda et al., 1995, 2000). At its southern extremity, it occurs as a network of veins and as small plutons; towards the North it forms high-level intrusions cutting across the Peninsular Gneisses and greenstone belts. The parallelism of batholith contacts with the strike of the surrounding greenstone belts indicates that the deformation which caused the elongate structure of the greenstones also guided the emplacement of the Closepet batholith (Newton 1990a). Several small discontinuous bands of high grade supracrustal rocks (quartzites – pelites - calc silicate – amphibolite - BIF association) are found along the periphery of the Closepet granite.

### Pavagada Area:

The studied area around Pavagada is located in the Central part of the EDC along the eastern boundary of the Closepet granite (Fig. 2). The lithologies in this corridor include TTG gneisses with discontinuous exposures or remnants of high grade supracrustal rocks (metapelites with minor calc-silicate rocks and amphibolites), Closepet granite and small linear gabbroic intrusions. The TTG occurs as polyphase gneisses along the boundary of Closepet granite and frequently found as enclaves within granite. They are migmatitic and traversed by prominent N20$^0$ E trending dextral shear bands and N30$^0$ W trending sinistral shear bands.

The high grade supracrustal rocks are mainly dark grey metapelites with minor calc-silicate rocks and amphibolites, mainly confined to interfering regional NNE trending dextral and NNW trending sinistral shear zones (Chardon et al., 2008). The studied pelitic rocks occur in an area bounded by latitude 14$^0$ 04’ 54’’ N - 14$^0$ 14’ 32’’ N and longitude 77$^0$ 17’ 25’’ E -77$^0$ 24’ 04’’ E, which are found as NE trending bouldery exposures along the eastern boundary of the Closepet batholith along Pavagada-Nagalmadke road, with large porphyroblasts of sillimanites with relict blades of kyanites (Fig. 3), bluish grey cordierite, green spinel and biotites. Sillimanite porphyroblasts measuring upto 15cm long and frequently shows random orientation. Occasionally garnet crystals are also observed. These metapelites are weakly migmatized and injected by tiny granitic veins (Fig. 4). Migmatization and injection of granite veins are contemporaneous with shearing. Thin film of melt found around sillimanite/kyanite porphyroblasts indicates development sillimanite/kyanite prior to migmatization.

Fig. 3. Metapelite showing large porphyroblasts of Sillimanite with relict blades of Kyanite (1km NE of Paluvalli area along Pavagada – Nagalmadke road).

Fig. 4. Migmatized metapelite injected by tiny granitic veins (1km NE of Paluvalli area along Pavagada – Nagalmadke road).

### Bidaloti area:

The area around Bidaloti lies along the eastern margin of Closepet granite about 5 km east of Koratagere where a variety of supracrustal rocks are exposed which are represented by quartzites, cordierite bearing pelites, minor bands of calc-silicate rocks and BIF associated basic igneous rocks (pyroxene granulites, amphibolites and hornblendite). These supracrustal rocks are surrounded by Peninsular gneisses which in turn are intruded by sheets of Closepet granite (Fig. 5).

Cordierite bearing metapelites are the most abundant lithounit of the area. These bands generally occur bordering the sillimanite bearing quartzites and are often interbanded with basic and calc-silicate rocks. Cordierite bearing pelitic band in the Bidaloti area can be traced over a distance of 2.5km, starting from about 0.5km south of Bidaloti village upto Bajanahalli. They are found as disconnected bands and patches. These metapelites show characteristic pitted appearance (Fig. 6) due to removal of biotites by weathering process. Towards north, these exposures are truncated by Closepet granite. The contact between cordierite bearing pelites and Closepet granite is not seen in field.

The eastern limb of this folded cordierite bearing metapelites band is exposed 0.5km SSE of Bidaloti village. Here, the cordierite bearing pelites are fine grained variety at the contact of ultramafic hornblendite but are coarse grained 75m away towards east. The contact between the two lithounits (ultramafic hornblendite and the metapelite) is rather sharp, and at the contact, the hornblendite is compact, fresh, coarse grained and contains abundant garnets, while the pelites are extremely fine grained that, they apparently resemble hornfels. The grain size of this band gradually increases and the rock becomes schistose to granular, but still highly melanocratic and compact. This band has an approximate width of 5m and one can notice small sheaths of orthoamphibole, bluish cordierite specks and biotite. With further increases in grain size and concomitant increase in felsic minerals, the rock becomes well foliated and is of banded nature with the felsic minerals constituting the leucocratic band.

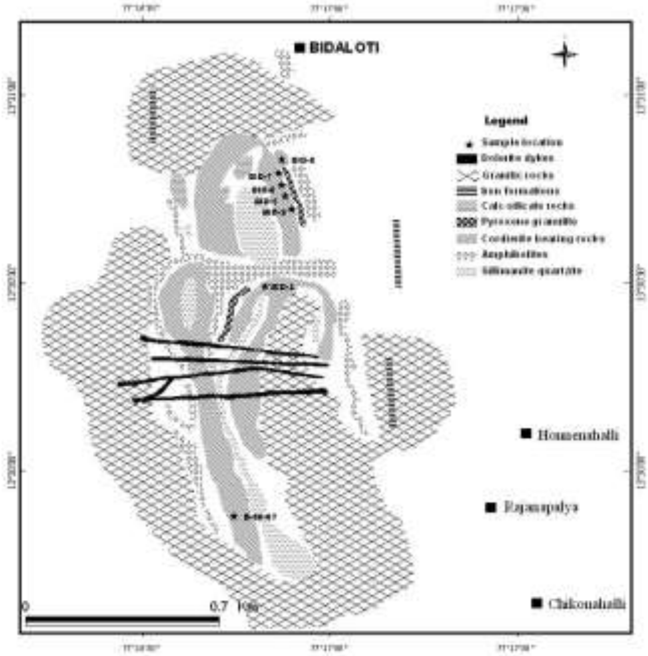

Fig. 5. Geological sketch map of Bidaloti area (modified after M. Jayananda, 1985).

Fig. 6. Bidaloti area Metapelite showing pitting appearance due to removal of biotites by weathering process (0.5 km S of Bidaloti).
.

**Bandihalli area:**

The Bandihalli area is situated on the western margin of the Closepet granite has a variety of metasedimentary lithologies. The main lithotypes of the area comprising of metapelites, quartzites, calc-silicate rocks and iron formations; amphibolites, actinolite schists, gneisses and dolerite dykes (Fig. 7).

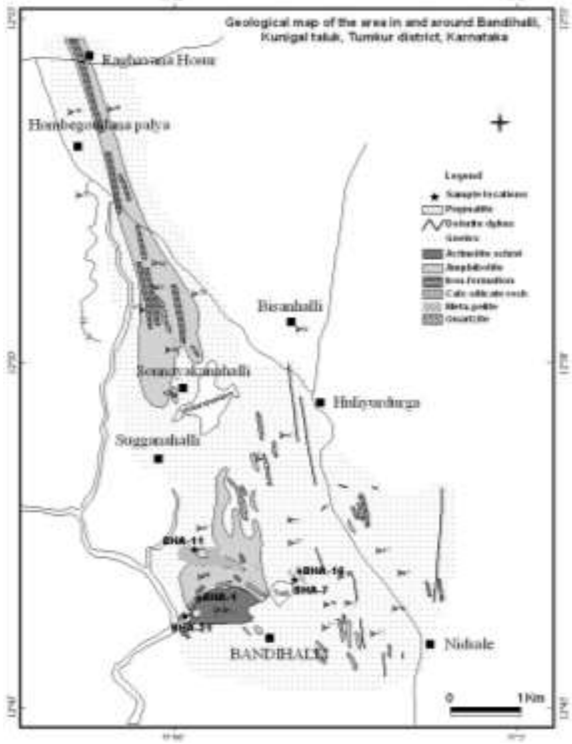

Fig. 7. Geological sketch map of Bandihalli area (modified after Mahabaleswar et al 1989).

Fig. 8. Metapelite showing well developed anthophyllite and biotite (about 200m E of Baiyrnayakanahalli).
.

These rocks are similar in terms of structure, metamorphism and migmatization with the Sargur supracrustals, but there is variation in lithotypes. While Sargur terrain predominantly contains K-Al rich metapelites, manganiferous horizons and various components of the layered ultramafic rocks (Janardhan et al., 1986), the Bandihalli area has Mg-Al rich pelites (Eunuse Akon unpublished thesis) and typical ultramafic-mafic complex are absent. This may be attributed to change in litho facies i.e. a reflection of difference in provenance (Ramakrishnan 1980) or because of restricted localization of the ultramafic and mafic complexes along a particular arcuate zone in the craton (Ramakrishnan et al., 1978). The metapelites of the area are represented by cordierite-anthophyllite-garnet-biotite schist (Fig. 8) and biotite-quartz-schist. These are widely exposed in the southern portions of the area and are sporadic in the northern portions. The striking feature of the metapelites is that most of the minerals are well developed and also show migmatitic character.

A cluster of enclaves of anthophyllite-cordierite-garnet-biotite schists are found extensively around Bairanayakanahalli and Doddakoppalu. These rocks contain well developed sheafs of anthophyllite and garnet. Porphyroblasts of garnets are mainly seen in the samples of Doddakoppalu. Garnetiferous-cordierite-quartz-biotite schist is exposed on a small hill to the north of Sonnayakanahalli. The rock is associated with iron formation and is highly weathered and its schistosity is due to alignment of biotite flakes.

**Duntur area:**

The area around Duntur forms the southern most extreme of the Closepet granite. The supracrustal rocks of the area are represented by quartzites, cordierite bearing metapelites, calc-silicate rocks, banded iron formations, Mn-horizons, amphibolites and basic granulites (Fig. 9). These rocks occur as enclaves within gneisses and charnockites. The metasediments occur as bouldery outcrops and are exposed in low laying mounds and nallah sections. Cordierite bearing metapelites occur as small thin, disconnected bands closely associated with quartzite, banded iron formations, Mn-garnetiferrous horizons, amphibolites and basic granulites. In the field, they are grey to bluish grey with pink tints, medium to coarse grained nature with a compositional banding. On weathered surfaces, the rock is whitish. The Dull white to cream coloured porphyroblasts of sillimanite are seen oriented parallel to foliation (Fig. 10). Pink coloured garnets and cordierite also occur as porphyroblasts as well as small round grains. Occasionally metapelites are migmatized to varying degree. The metapelites outcrops trend NNW and dips $35^0$-$48^0$ towards east.

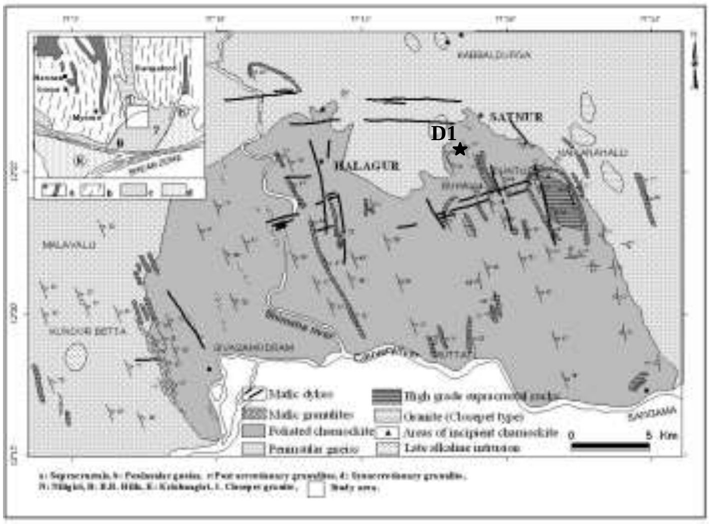

Fig. 9. Geological map of Duntur area (modified after Mahabaleswar et al 1995).

Fig. 10. Metapelite showing dull white to cream coloured porphyroblasts of sillimanite oriented parallel to the foliation (0.5 km SW of Duntur).

.

## III. GEOCHEMISTRY

**Analytical techniques:**

The Major elements were analyzed by XRF (Phillips, Holland) and trace & Rare Earth Elements were analyzed by ICP-MS ELAN DRC II (Perkin-Elmer, Sciex, USA) at NGRI, Hyderabad. Whole rock Sm-Nd and Rb-Sr isotopic analysis for representative samples of metapelites were carried out by using TIMS (Triton, Thermos Finnigan) at IIT, Roorkee.

***Sample preparation, instrumentation and operating parameters:***

*a. X-Ray fluorescence spectrometry*

Collapsible aluminium cups were filled with 9 gm of boric acid, which acts as binding material. 1 gm of ~ 200 mesh homogenized sample powder was sprayed upon it by covering the boric acid uniformly and about 15 tons of pressure was applied using Herzog hydraulic press (H/100) to obtain a pressed pellet of 40 mm diameter. The samples were analyzed for major elemental compositions by Phillips Pw 1400 microprocessor controlled wavelength dispersive, sequential X-Ray Fluorescence spectrometer (Phillips, Holland). The system was interfaced to a Phillips P851 online minicomputer for preparing calibration curves relating the concentration and intensity levels in a standard as well as the unknown samples after due matrix corrections. Software available in the computer was able to take care of dead time; background and line overlap corrections after regression and converting the counts into correction with the help of the calibration curves finally giving the output directly as concentration in oxide percentages (or) in PPm as required. A spinner was used to spin the samples inside the spectrometer while measuring to have uniform counts. Certain elements were analyzed using a Rhodium target X-ray tube while a Chromium X-ray target tube estimated Na, Al and Mg since the concentration levels of these elements were very low. All the elements were estimated under a high vacuum condition (10-6 Torr). The major and minor elemental data estimated by XRF are reproducible with a precision range of ± 5 %.

### *b. Inductively coupled plasma quad-mass spectrometer*

The trace and rare earth elemental analysis of the rock samples were carried out by ICP-MS-ELAN DRC II (Perkin - Elmer, Sciex, USA). The instrument is equipped with Dynamic reaction cell and other advancements leading to extremely low background, better sensitivity and striking improvement in measurement precision which takes the detection limits for the most of the elements in the periodic table to pg/ml (ppt) and fg/ml (ppq) levels. The fine rock powders and standards were analyzed for nearly 30 trace elements, including the Rare Earth Elements (REE) and the High Field Strength Elements (HFSE), using an Inductively Coupled Plasma Mass Spectrometer (ICP-MS).

0.05g of the sample was taken in 14 mal screw capped PFA Teflon beakers (Savillex beakers). 10ml of acid mixture (7:3:1; HF-analar grade, $HNO_3$-quartz distilled 14 N $HNO_3$ and $HClO_4$-AR-grade) was added to each sample, standard and a blank beaker (for process blank). The samples were then swirled vigorously. The beakers were capped tightly and kept aside at room temperature for about 48hrs for digestion. 1ml of 5µgml-1 Rh solution (internal standard) was added by a fine pipette. The beakers were warmed on a hot plate for about 1 hour, with the caps loosely on. The solution was evaporated at $180^0$ C till the last drop and further heated at approximately $210^0$C to dryness until the $HClO_4$ vapors were expelled completely. Then, the residues were dissolved using 10ml of 1:1 $HNO_3$ and kept on a hot plate for 10 minutes at gentle heat ($70^0$ C) to obtain a clear solution. Finally, the solution was made to 250 ml using Milli-Q (18.2 MΩ) water and stored in pre-cleaned screw capped PVC bottles for analysis.

A Perkin Elmer SCIEX, Model ELAN ® DRC II ICP-MS in National Geophysical Research Institute (NGRI), was used for trace element analysis of the rock samples, standards and the process blank. The sample introduction system consisted of a standard Meinhard nebulizer with a cyclonic spray chamber. All quantitative measurements were performed using instrument software, which used knowledge driven routines in combination with numerical calculations to perform an automated interpretation of the whole spectrum, several well-known isobaric interferences were programmed and the corrections applied automatically. A calibration procedure using an internal standard, subtraction and reference to a well-defined calibration curve for each element based on multiple international rock standards and gravimetric element solutions were used in processing of the analytical data similar to those described in Balaram and Gnaneshwar Rao, 2003.

Solutions containing > 5% v/v acid result in substantial erosion of the cone surface and in the geometry of the aperture itself (Brenner and Zander, 1996). Hence, in the present investigations, only solutions of 0.02% m/v TDS and <2% v/v $HNO_3$ were nebulized. The detection limits for all the trace elements and REE were found to be in the range 0.001 to 0.010ng/g. Replicate analyses of samples and reference rock standards were also carried out all through the analysis of samples to cross check the results and instrument performance. Procedural blank also was run to rule out any possibility of contamination from the reagents. Overall, an accuracy of better than ± 5% was obtained for most analysis with precision of better than ±6% RSD. However, precision was highly dependent on the absolute concentration in the material. Determinations made close to the quantification limit of ICP-MS, gives poorest precision as expected, while more consistent results were obtained for elements at higher concentrations, many yielding RSD of better than ± 5%.

### *c. Thermal Ionization Mass Spectrometer (TIMS)*

Sample weighing and dissolution: ~100mg of representative samples (whole rock powder) were weighted on a precision electronic balance and transferred into ultra-cleaned 14ml PFA Teflon vessels (Savillex). Add 3ml HF (48%) and 1ml of highly purified $HNO_3$ acid to Teflon vessel containing sample. Place the tightly capped Teflon vessel on hot plate for 48 hours. After 48 hours, open the lids slowly (when the temperature of the vessel reaches to room temperature) and the solution was evaporated to dryness to expel silica, and then add 10 drops of $HNO_3$ and evaporated to dryness to ensure complete expulsion of $SiO_2$. Add 2 ml of concentrated HCl, cap it tightly and place it on hot plate for 12 hours. After 12 hours, open the lids slowly (when the temperature of the vessel reaches to room temperature) and check, whether the solution is clear or not. If the solution is not clear, once again add 1:3 HNO3: HCl, cap it tightly and place it on hot plate for 12 hours. After 12 hours, open the lids slowly (when the temperature of the vessel reaches to room temperature) and check, whether the solution is clear or not. If the solution is not clear, repeat the same process twice and finally the sample was dissolved in 2N HCl.

Spiking and centrifuging: Spike is a solution that contains a known concentration of a particular element in which natural isotopic composition has been altered by the enrichment of one of its naturally occurring isotopes. This technique can be applied to any element with two or more naturally occurring isotopes, provided a spike is enriched in one of the isotopes of that element is available. In the present study $^{87}$Rb (Granite), $^{84}$Sr (Granite) and $^{149}$Sm-$^{150}$Nd (Basalt) spikes were used for the Isotopic dilution analysis of Rb, Sr and Sm-Nd. Samples were spiked accurately by adding appropriate amounts of the spike to the sample dissolved in 2N HCl solution by weight. The mixture was kept aside over 30 minutes for homogenization. Further, these spiked samples were evaporated to complete dryness on a hot plate at approximately $90^0$ C. The residue was re-dissolved in 1ml 2N HCl and centrifuged for 5-10 minutes at maximum speed.

Ion exchange chromatography: The supernatant liquid was used for chromatographic separation of Rb, Sr and REE, as described below. Ion exchange chromatography refers to any exchange method involving the distribution of components between a fixed (stationary) and a moving (mobile) phase. The latter is also called the eluent. The process by which an eluent makes a compound move along a column is called elution. In the present study, the method adopted involves standard cation exchange chromatography, where a cation exchange resin such as Bio Rad AG 50W-X8, 200-400 mesh forms the stationary phase and HCl of certain specific normality (2N HCl for Rb, Sr separation and 6N HCl for REE separation) forms the eluent. The resin is normally packed in a suitable glass tube (in the present case columns were made from fused pure quartz) columns held vertically, and the sample solution is loaded on the top of the column. The sample is then eluted by washing its ionic components through the columns using a suitable solvent at a controlled rate. Ions are separated from one another due to difference in their affinity towards the ion exchange resin. The more strongly an ion is attracted to the resin, the larger the volume or the concentration or normality of the eluent required to wash that ion out of the ion exchange column. Rb, Sr and REE were colleted in pre-cleaned Savillex vials and allowed to dry completely on hot plate at $90^0$ C temperatures. Separation of Sm, Nd from REE was done by using secondary column techniques.

Filament welding and degassing: The filaments used during this analysis were made of high melting pure Tungsten (W) (used as evaporation filament) and Rhenium (Re) (used as ionization filament). The filaments were prepared by welding the cut pieces of W/Re – 0.001” thick, 0.3” wide and 0.4-0.7” long in the poles of the filament assembly with the help of spot welder. Single filaments were used for loading Rb and Sr fraction only (in single filament we will use only tungsten filament as evaporation filament). Double filaments were used for loading Sm and Nd fraction (in double filament we will tungsten filament as evaporation filament and Rhenium filament as ionization filament). These filaments were degassed in degassing unit to remove the gasses present in the filament which can cause interference with the ionization process.

Sample loading: The degassed filaments were then transferred to sample loading chamber. The sample loading chamber consists of a sample loading unit which contains filament slots to position the filaments. One micro liter of $TaF_5$ is used as base ( for Rb, Sr, Sm, Nd fractions) on the W-filament which acts as adhesive surface for sample and also removes the organic impurities from the sample and dried at less than 0.5 amps current. Further add one micro liter of $H_3PO_4$ as activator (only for Sm and Nd fractions) and dried at less than 0.9 amps current. To the Rb, Sr, Sm and Nd fraction, 2 micro liter of MQ water was added and the sample was loaded with micro-tip fitted in the pipette over the spot of partially dried $TaF_5$ or $H_3PO_4$(use separate micro tips for each individual samples). The filament loaded with sample was heated to dryness by increasing the filament current gradually from 0.9 amps to a dull red state and maintained for about 10seconds until dense fumes were expelled and then brought back to zero. And the turret assembly of upto 21 sample loaded dried filaments is loaded into the source housing of the TIMS.

Mass spectrometric analysis: Rb, Sr, Sm and Nd ratios were measured using a multi collector programme. Typical Rb, Sr, Sm and Nd run for about 30minutes, 2 hours, 45 minutes and 1 hour 30 minutes respectively.

**Major elements:**

The major element analyses of the 15 studied metapelites are given in Table. I. Metapelites of the Pavagada area exhibit $SiO_2$ content ranging from 53.87 to 63.88wt. % and $Al_2O_3$ from 15.27 to 25.19wt. %, $Fe_2O_3$ from 8.45 to 10.02 and MgO from 5.82 to 7.06wt. % (See Table. I). Majority of the samples of Pavagada area contain CaO less than 1wt. %, where $Na_2O$ & $K_2O$ are less than 2%.

Bidaloti metapelites exhibit $SiO_2$ ranging from 50.27 to 68.84wt. % and $Al_2O_3$ from 9.85 to 17.23wt. % (See Table. I). Compared to pelites from Pavagada & Duntur, Bidaloti pelites have lower $Al_2O_3$, higher $Fe_2O_3$ and MgO ($Fe_2O_3$ varies from 8.42 – 15.97wt. % and MgO varies from 8.02 – 15.88wt. %).

Metapelites of the Bandihalli area exhibit $SiO_2$ content varies from 55.54 to 69.83wt. %, MgO from 6.42 to 14.33wt. %, $Al_2O_3$ from 10.33 to 10.75wt. %, $Fe_2O_3$ from 11.76 to 15.35 and CaO from 0.25 to 0.45wt. % with very low concentrations of $K_2O$ and $Na_2O$ compared to Bidaloti and Pavagada area (See Table. I).

Metapelite from the Duntur area has 57.42wt. % of $SiO_2$ and is rich in $Al_2O_3$ (22.61wt. %), $Fe_2O_3$ (8.19 wt. %), MgO (5.49wt. %) and $TiO_2$ (1.03wt. %) (See Table. I).

The average major element $TiO_2$, $Fe_2O_3^T$, MnO and MgO values of metapelites from Pavagada, Bidaloti, Bandihalli and Duntur area were, higher than, those of NASC and PAAS ($TiO_2$= 0.7-1 wt. %, $Fe_2O_3$ =5.67-6.5 wt. %, MnO =0.06-0.11wt. % and MgO =2.2-2.86wt. %) where as other major elements $SiO_2$, CaO and $K_2O$ were lower than, those of

NASC and PAAS ($SiO_2$=62.8-64.8wt. %, CaO=1.3-3.63wt. % and $K_2O$=3.7-3.97wt. %) (See Table. I). But average $Al_2O_3$ values of Pavagada and Duntur metapelites were higher than NASC and PAAS values ($Al_2O_3$=16.9-18.9wt. %), where as Bidaloti and Bandihalli metapelites shows lower values.

Table. I. Major elements data of the studied metapelites.

| **Location** | **Pavagada** | | | | | | | | **Bandihalli** | | |
|---|---|---|---|---|---|---|---|---|---|---|---|
| **Sample No.** | **P-1** | **P-10** | **P-11** | **P-14** | **P-15** | **P-16** | **P-18** | **Avg.** | **BHA-7** | **BHA-11** | **Avg.** |
| **$SiO_2$** | 55.63 | 57.82 | 60.09 | 54.46 | 55.54 | 53.87 | 63.88 | 57.33 | 69.83 | 55.54 | 62.68 |
| **$Al_2O_3$** | 25.19 | 22.00 | 18.96 | 21.01 | 24.61 | 24.48 | 15.27 | 21.65 | 10.33 | 10.75 | 10.54 |
| **$Fe_2O_3$** | 8.45 | 8.54 | 8.98 | 10.02 | 9.81 | 8.70 | 8.50 | 9.00 | 11.76 | 15.35 | 13.56 |
| **MnO** | 0.07 | 0.09 | 0.09 | 0.10 | 0.09 | 0.09 | 0.08 | 0.09 | 0.08 | 0.20 | 0.14 |
| **MgO** | 5.95 | 5.82 | 6.33 | 7.05 | 7.06 | 5.99 | 5.84 | 6.29 | 6.42 | 14.33 | 10.38 |
| **CaO** | 0.58 | 0.69 | 1.82 | 1.59 | 0.20 | 0.67 | 1.56 | 1.01 | 0.25 | 0.45 | 0.35 |
| **$Na_2O$** | 1.21 | 1.75 | 1.61 | 1.88 | 0.51 | 1.53 | 1.31 | 1.40 | 0.28 | 0.36 | 0.32 |
| **$K_2O$** | 1.53 | 1.74 | 1.44 | 1.46 | 1.60 | 1.88 | 1.53 | 1.60 | 1.03 | 0.32 | 0.67 |
| **$TiO_2$** | 0.97 | 0.93 | 0.99 | 1.12 | 1.07 | 0.99 | 0.93 | 1.00 | 0.91 | 0.59 | 0.75 |
| **$P_2O_5$** | 0.03 | 0.03 | 0.04 | 0.03 | 0.01 | 0.04 | 0.03 | 0.03 | 0.08 | 0.15 | 0.12 |
| **Total** | 99.60 | 99.41 | 100.35 | 98.72 | 100.52 | 98.23 | 98.93 | 99.40 | 100.97 | 98.04 | 99.51 |
| **CIA** | 84.29 | 78.55 | 71.64 | 73.52 | 89.32 | 80.96 | 69.65 | 78.28 | 83.54 | 85.99 | 84.77 |
| **CIW** | 89.24 | 84.20 | 76.13 | 77.81 | 95.31 | 86.81 | 75.35 | 83.55 | 91.84 | 88.40 | 90.12 |
| **TiO2/Al2O3** | 0.04 | 0.04 | 0.05 | 0.05 | 0.04 | 0.04 | 0.06 | 0.05 | 0.09 | 0.05 | 0.07 |
| **SiO2/Al2O3** | 2.21 | 2.63 | 3.17 | 2.59 | 2.26 | 2.20 | 4.18 | 2.75 | 6.76 | 5.16 | 5.96 |
| **K2O/Na2O** | 1.27 | 0.99 | 0.90 | 0.77 | 3.11 | 1.23 | 1.17 | 1.35 | 3.67 | 0.88 | 2.27 |

Table. I. Continue……….

| **Location** | **Bidaloti** | | | | | | **Duntur** | | **PAAS** | **NASC** |
|---|---|---|---|---|---|---|---|---|---|---|
| **Sample No.** | BID-2 | BID-05 | BID-07 | BID-09 | B-06-07 | Avg. | D-1 | | | |
| **$SiO_2$** | 53.68 | 57.87 | 54.08 | 68.84 | 50.27 | 56.95 | 57.42 | $SiO_2$ | 62.8 | 64.8 |
| **$Al_2O_3$** | 11.16 | 9.85 | 17.23 | 12.00 | 14.80 | 13.01 | 22.61 | $Al_2O_3$ | 18.9 | 16.9 |
| **$Fe_2O_3$** | 15.20 | 14.47 | 15.84 | 8.42 | 15.97 | 13.98 | 8.19 | $FeO^T$ | 6.5 | 5.67 |
| **MnO** | 0.30 | 0.17 | 0.23 | 0.08 | 0.23 | 0.20 | 0.07 | MnO | 0.06 | 0.11 |
| **MgO** | 15.88 | 13.95 | 10.81 | 8.02 | 15.29 | 12.79 | 5.49 | MgO | 2.2 | 2.86 |
| **CaO** | 0.73 | 0.32 | 0.24 | 0.24 | 0.52 | 0.41 | 0.76 | CaO | 1.3 | 3.63 |
| **$Na_2O$** | 0.42 | 0.18 | 0.37 | 0.19 | 0.36 | 0.30 | 0.99 | $Na_2O$ | 1.2 | 1.14 |
| **$K_2O$** | 0.41 | ND | 0.04 | 1.55 | 0.28 | 0.57 | 1.89 | $K_2O$ | 3.7 | 3.97 |
| **$TiO_2$** | 1.07 | 1.11 | 1.17 | 0.81 | 1.11 | 1.05 | 1.03 | $TiO_2$ | 1 | 0.7 |
| **$P_2O_5$** | 0.18 | 0.13 | 0.02 | 0.14 | 0.19 | 0.13 | 0.01 | $P_2O_5$ | 0.16 | 0.13 |
| **Total** | 99.03 | 98.03 | 100.04 | 100.28 | 99.02 | 99.28 | 98.48 | Total | 97.82 | 99.91 |
| **CIA** | 82.01 | - | 94.03 | 83.28 | 88.97 | 87.07 | 81.68 | | | |
| **CIW** | 84.74 | 91.85 | 94.26 | 94.21 | 90.65 | 91.14 | 88.21 | | | |
| **TiO2/Al2O3** | 0.10 | 0.11 | 0.07 | 0.07 | 0.07 | 0.08 | 0.05 | | | |
| **SiO2/Al2O3** | 4.81 | 5.88 | 3.14 | 5.73 | 3.40 | 4.59 | 2.54 | | | |
| **K2O/Na2O** | 0.98 | - | 0.11 | 8.16 | 0.79 | 2.55 | 1.91 | | | |

Pavagada and Duntur area metapelites were relatively similar in their major element chemistry and have higher concentration of $Al_2O_3$ ($Al_2O_3$ content varies from 18.96 to 25.19wt. %, except P-18) because of higher modal sillimanite abundance, whereas metapelites from Bidaloti and Bandihalli area were similar and have higher concentration of MgO (average MgO content varies from 10.38-12.79wt. %) because of higher modal cordierite abundance.

No systematic variations between most of the major oxides with $SiO_2$ and $Al_2O_3$ were observed (Fig. 11 and Fig. 12). There are clear positive correlations between $K_2O$ content and the abundances of $Al_2O_3$, Cs, Ba, total REE, Th, U (Fig. 13) and possibly Sr and Pb, suggesting the absolute abundances of these elements are primarily controlled by the amount of the dominant original clay mineral. In majority of the studied metapelites, $Al_2O_3$wt. % decreases with increasing $SiO_2$wt. % (Fig. 14), the high silica can be attributed to the addition of quartz subsequently or due to the mixing of original clay with arenaceous material.

The $SiO_2/Al_2O_3$ and $K_2O/Na_2O$ ratios have been considered to reflect evolutionary changes in the compositions of continental crust (Viezer 1973; Schwab 1978) and province (Condie and Wronkewicz 1990a). Average $SiO_2/Al_2O_3$ ratios of Pavagada, Duntur, Bidaloti and Bandihalli pelites are 2.75, 2.54, 4.59 and 5.96 respectively. Majority of the studied pelites exhibit elevated $K_2O/Na_2O$ ratios (>1) which are broadly comparable with the reported averages for the pelites of the Archaean high-grade terrains elsewhere in the world. However, a few samples show low $K_2O/Na_2O$ ratios.

On $K_2O/Na_2O$ Vs $SiO_2/Al_2O_3$ diagram (Fig. 15) the majority of the Pavagada pelites plot in the overlap-area of shale and greywacke fields (Condie et al., 1991) with $K_2O/Na_2O$ ratios (0.77 – 3.11) and $SiO_2/Al_2O_3$ ratios (2.20 – 4.18) whereas, Bidaloti pelites congregate within the greywacke field of Condie et al., 1991 with $K_2O/Na_2O$ ratios (0.11 – 0.98) and $SiO_2/Al_2O_3$ ratios (3.14 – 4.81), except BID-09. On the other hand Bandihalli pelites, BHA-11 plot within the greywacke region ($K_2O/Na_2O$=0.88, $SiO_2/Al_2O_3$ =5.16) and BHA-07 plot outside the greywacke/shale field ($K_2O/Na_2O$=3.67, $SiO_2/Al_2O_3$ = 6.76) of Condie et al., 1991. The studied Duntur metapelite plot within the shale field of Condie et al., 1991 with $K_2O/Na_2O$ ratio 1.91 and $SiO_2/Al_2O_3$ ratio 2.54.

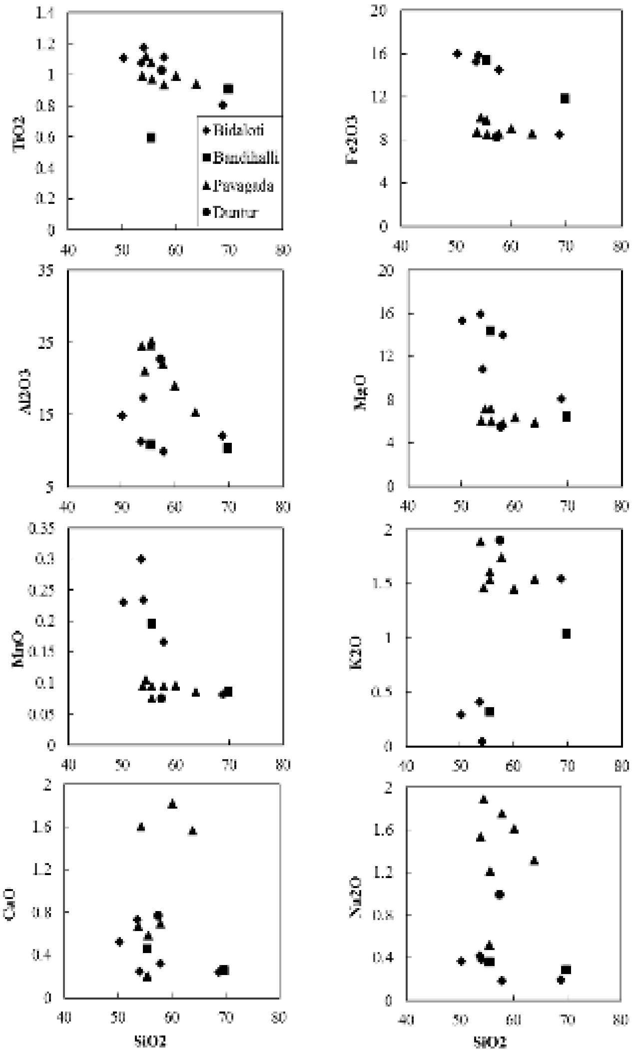

Fig. 11. Major oxides (in wt %) v/s $SiO_2$ diagram.

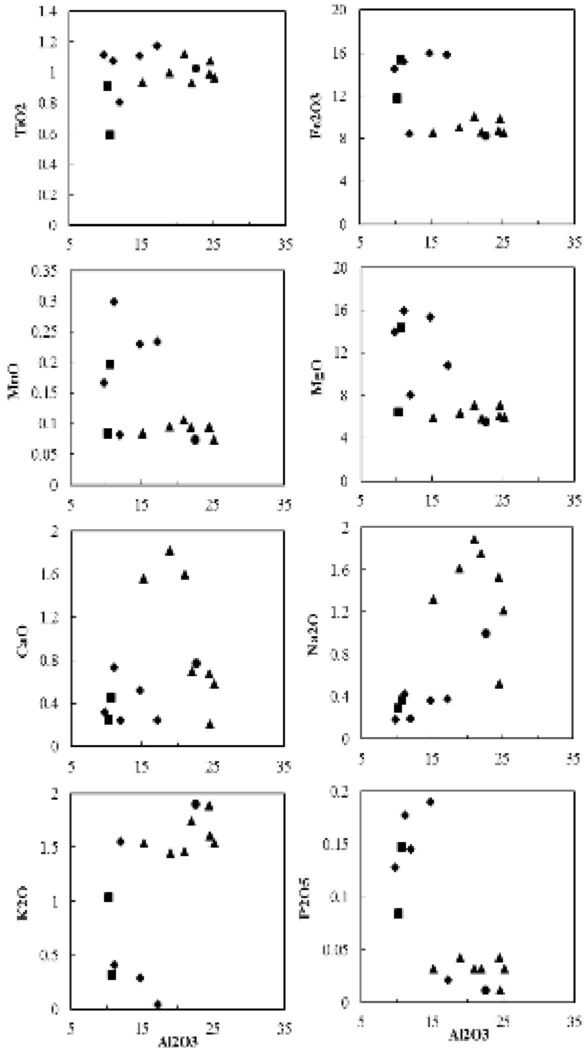

Fig. 12. Major oxides (in wt %) v/s $Al_2O_3$ diagram.

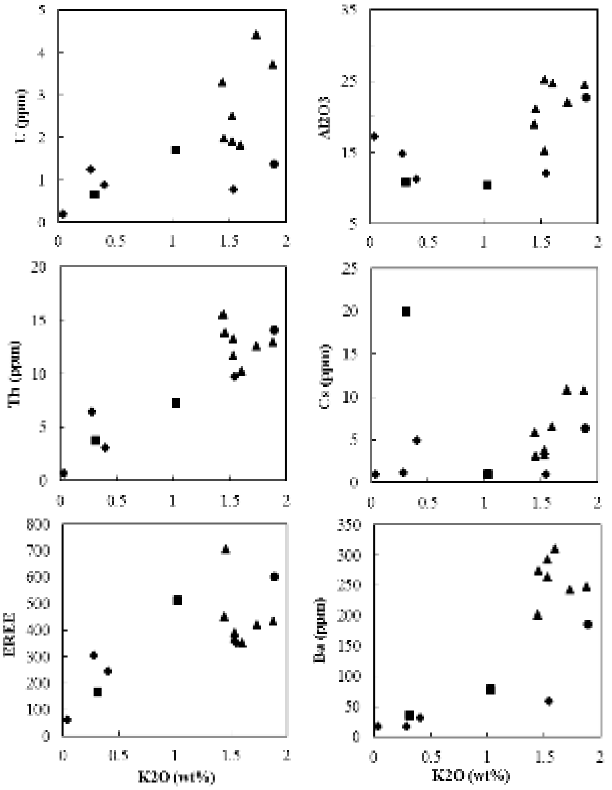

Fig. 13. Plots against various elements against $K_2O$ content

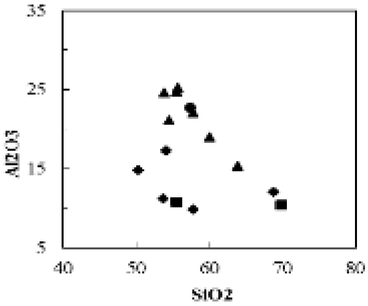

Fig. 14. Plot of $SiO_2$ against $Al_2O_3$.

.

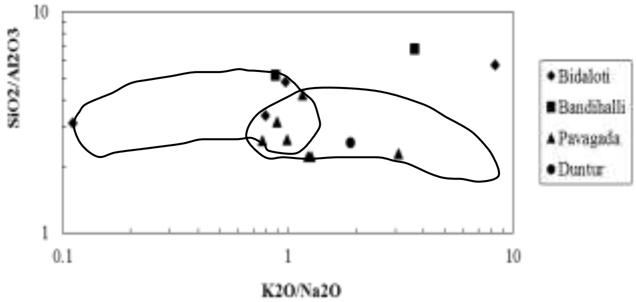

Fig. 15. $K_2O/Na_2O$ Vs $SiO_2/Al_2O_3$ diagram.

.

**Weathering:**

Virtually all studies of weathering have dealt exclusively with weathering profiles, but the quantitative assessment of weathering effects on sedimentary rocks is comparatively recent. Weathering in source areas can cause relative depletion of alkali and alkaline earth elements and corresponding enrichment of $Al_2O_3$ (and $TiO_2$) in terrigenous sedimentary rocks. The extent of source area weathering (i.e., chemical processes that affected protoliths before erosion, transport and sedimentation) can be quantified with the Chemical Index of Alteration (CIA: Nesbitt and Young, 1989) or the Chemical Index of Weathering (CIW: Harnois, 1988) using molecular proportions of major elements. Unweathered basalts and granitoids are characterized by CIA values of 30-45 and 45-55, respectively, while average shales have CIA values of 45 to 70.

The calculated CIA values of pelites of Pavagada range from 70 – 89, Bidaloti from 82 – 94, Bandihalli from 84 – 86 and a single pelite sample from Duntur has a value of 82, which are more than PAAS (CIA=70). Highly variable CIA values and low contents of Ca and Na in the metapelites of the present study indicate variable and locally moderate to intense weathering of the source rocks.

The calculated CIW (Chemical Index of Weathering) values of pelites of Pavagada range from 75– 95, Bidaloti from 85 – 94, Bandihalli from 88 – 92 and a single pelite sample from Duntur has a CIW value of 88, which also indicates moderate to intense weathering.

**Trace elements:**

During the past decade, the study of trace element abundances (particularly REE) in sedimentary rocks has revealed considerable information about the composition and evolution of the continental crust (Taylor and McLennan, 1981a, 1981b; McLennan et al., 1980). In addition, important information about the provenance of specific sedimentary sequences can be derived from geochemical studies (e.g. Nathan, 1976; Jenner et al., 1981; Bhatia and Taylor, 1981). Relating sedimentary compositions to that of source rocks requires caution because many secondary processes, including weathering, sorting, diagenesis and metamorphism, can affect the chemistry. Elements which are relatively insoluble in natural waters are transferred almost quantitatively into clastic sedimentary rocks during weathering and recycling and thus provide the best information regarding provenance. The most useful elements include the rare earth elements, Th and Sc (Wildeman and Haskin, 1973; McLennan et al., 1980; Taylor and McLennan, 1981b; McLennan, 1981).

An important discovery has been that the REE patterns of post-Archaean sedimentary rocks have remained essentially constant (Nance and Taylor, 1976; McLennan et al., 1979; McLennan and Taylor, 1980a). The average pattern is characterized by a significant negative Eu-anomaly. The presence of a negative Eu-anomaly in post-Archaean sedimentary rocks, and hence in the upper crust, is strong evidence that intracrustal melting is a major, if not dominant, process in differentiating the continental crust (Taylor and McLennan, 1981a, b).The average post-Archaean sedimentary REE pattern is consistent with the granodioritic upper crust composition suggested by large-scale sampling programs in shield areas (Shaw et al., 1967; Eade and Fahrig, 1971).

Archaean sedimentary rocks have very different REE patterns from post-Archaean sedimentary rocks (Taylor and McLennan 1985). These rocks generally have lower total REE abundances (ΣREE), commonly less fractionated patterns (i.e., lower La/Yb) and, most importantly, they almost invariably lack any significant negative Eu-anomaly (Wildeman and Condie, 1973; Nance and Taylor, 1977; Bavinton and Taylor, 1980; McLennan et al., 1983, 1984). These data support the idea of a more mafic crust (less enriched in incompatible elements) during the Archaean, whose differentiation was less affected by shallow intracrustal melting (Taylor and McLennan, 1981a, b, c).

The concentrations of selected trace elements in the studied metapelites are given in Table. I I.

***Large Ion Lithophile Elements (LILE):***

Large ion lithophile elements such as Rb, Sr, Ba and Cs behave similarly to related major elements during weathering processes. Like $K_2O$, Rb and Cs will be incorporated into clays during chemical weathering. In contrast, CaO, Sr and $Na_2O$ tend to be leached (Nesbitt et al., 1980). Ca, Na along with Rb and Cs are mainly controlled by feldspars, so depletion of Ca, Na, Rb and Cs in the samples may suggest depletion of feldspar in studied samples. The absence of feldspar can be explained either by (i) removal of feldspar by post-depositional dissolution or through weathering in the source area or (ii) by their depletion in the source rocks.

A great deal of variability exists in the contents of LILE in the studied metapelites, due perhaps to the mobility of these elements during weathering, diagenesis and medium to high grade metamorphism.

Pavagada and Duntur area metapelites shows higher concentration of Th, U, Rb, Sr and Ba i.e. Th content varies from 10.22-15.55ppm, U from 1.36-4.42ppm, Rb from 51.19-146.16, Sr from 86.37-264.44ppm and Ba from 185.78-309.9ppm, whereas, Bidaloti and Bandihalli area metapelites shows intermediate to lower concentration of Th, U, Rb, Sr and Ba i.e. Th content varies from 0.67-9.72ppm, U from 0.18-1.68ppm, Rb from 2.51-42.19, Sr from 6.84-10.09ppm and Ba from 10.47-77.88ppm.

Table. II. Trace elements data of the studied metapelites.

| ***Sample No.*** | ***P-01*** | ***P-10*** | ***P-11*** | ***P-14*** | ***P-15*** | ***P-16*** | ***P-18*** | ***Avg.*** | ***D-1*** |
|---|---|---|---|---|---|---|---|---|---|
| ***Sc*** | 37.69 | 34.86 | 29.697 | 40.31 | 41.793 | 35.88 | 28.49 | 35.53 | 35.3 |
| ***V*** | 274 | 253.7 | 244.08 | 318.8 | 232.27 | 282.6 | 223.1 | 261.2 | 235.3 |
| ***Cr*** | 759 | 636.6 | 724.62 | 712 | 853.32 | 630.1 | 685.6 | 714.5 | 582.2 |
| ***Co*** | 62.4 | 56.95 | 67.973 | 69.32 | 71.787 | 59.11 | 61.48 | 64.15 | 54.34 |
| ***Ni*** | 305.7 | 269.9 | 289.27 | 321.1 | 335.03 | 291.6 | 273.9 | 298.1 | 261.2 |
| ***Cu*** | 50.74 | 42.18 | 70.064 | 69.99 | 22.379 | 47.64 | 41.07 | 49.15 | 56.81 |
| ***Zn*** | 72.71 | 74.55 | 99.151 | 90.05 | 131.33 | 124.7 | 76.64 | 95.59 | 91.48 |
| ***Ga*** | 35.34 | 34.2 | 30.256 | 35.74 | 39.391 | 34.4 | 26.09 | 33.63 | 25.98 |
| ***Rb*** | 64.11 | 105.6 | 57.542 | 55.99 | 76.131 | 103.7 | 51.2 | 73.47 | 146.2 |
| ***Sr*** | 244.3 | 221.3 | 150.74 | 241.2 | 86.375 | 264.4 | 120.3 | 189.8 | 105 |
| ***Y*** | 11.62 | 15.13 | 16.186 | 16.98 | 10.702 | 14.07 | 13.99 | 14.1 | 54.56 |
| ***Zr*** | 121.9 | 123.1 | 286.36 | 174.6 | 163.81 | 135.7 | 209.2 | 173.5 | 200.8 |
| ***Nb*** | 12.17 | 21.56 | 13.266 | 13.91 | 12.708 | 13.27 | 12.33 | 14.17 | 67.79 |
| ***Cs*** | 3.754 | 10.8 | 5.795 | 3.065 | 6.432 | 10.73 | 3.145 | 6.246 | 6.292 |
| ***Ba*** | 263.4 | 242 | 201.52 | 273.4 | 309.9 | 247.7 | 291.8 | 261.4 | 185.8 |
| ***Hf*** | 3.654 | 3.69 | 8.282 | 5.189 | 4.714 | 3.954 | 6.134 | 5.088 | 5.999 |
| ***Ta*** | 1.233 | 3.142 | 1.17 | 1.2 | 0.827 | 1.311 | 1.528 | 1.487 | 3.718 |
| ***Pb*** | 11.42 | 24.45 | 10.603 | 9.441 | 6.834 | 11.9 | 22.02 | 13.81 | 11.23 |
| ***Th*** | 11.65 | 12.57 | 15.556 | 13.81 | 10.221 | 12.93 | 13.26 | 12.86 | 14.07 |
| ***U*** | 2.508 | 4.422 | 3.303 | 1.978 | 1.812 | 3.716 | 1.894 | 2.805 | 1.365 |
| ***La*** | 38.75 | 40.06 | 43.835 | 75.04 | 35.726 | 41.64 | 34.14 | 44.168 | 44.91 |
| ***Ce*** | 67.77 | 72.2 | 74.989 | 129.7 | 61.944 | 73.92 | 60.2 | 77.238 | 79.76 |
| ***Pr*** | 8.055 | 8.641 | 9.039 | 15.43 | 7.378 | 8.933 | 7.206 | 9.240 | 9.579 |
| ***Nd*** | 29.02 | 31.59 | 32.95 | 55.13 | 27.2 | 33.32 | 26.94 | 33.736 | 35.2 |
| ***Sm*** | 6.043 | 6.589 | 6.627 | 9.689 | 5.537 | 6.938 | 5.62 | 6.720 | 7.706 |
| ***Eu*** | 1.936 | 1.764 | 1.963 | 2.91 | 1.161 | 1.725 | 1.605 | 1.866 | 1.724 |
| ***Gd*** | 5.031 | 5.377 | 5.586 | 7.909 | 4.361 | 5.745 | 4.756 | 5.538 | 7.62 |
| ***Tb*** | 0.769 | 0.87 | 0.904 | 1.11 | 0.679 | 0.886 | 0.771 | 0.856 | 1.609 |
| ***Dy*** | 3.268 | 3.835 | 4.2 | 4.604 | 2.951 | 3.905 | 3.679 | 3.777 | 9.949 |
| ***Ho*** | 0.488 | 0.613 | 0.666 | 0.702 | 0.455 | 0.609 | 0.575 | 0.587 | 2.046 |
| ***Er*** | 1.135 | 1.486 | 1.639 | 1.639 | 1.133 | 1.412 | 1.51 | 1.422 | 5.718 |
| ***Tm*** | 0.151 | 0.218 | 0.264 | 0.227 | 0.153 | 0.194 | 0.236 | 0.206 | 0.941 |
| ***Yb*** | 0.86 | 1.264 | 1.7 | 1.457 | 0.922 | 1.093 | 1.599 | 1.271 | 5.363 |
| ***Lu*** | 0.148 | 0.221 | 0.315 | 0.269 | 0.169 | 0.195 | 0.288 | 0.229 | 0.881 |
| ***ΣREE*** | 163.4 | 174.7 | 184.68 | 305.8 | 149.77 | 180.5 | 149.1 | 186.86 | 213 |
| ***(La/Yb)***$_N$ | 30.444 | 21.414 | 17.424 | 34.804 | 26.184 | 25.742 | 14.427 | 24.348 | 5.659 |
| ***Eu/Eu**** | 1.073 | 0.906 | 0.986 | 1.016 | 0.722 | 0.835 | 0.949 | 0.927 | 0.688 |
| ***(La/Sm)***$_N$ | 4.036 | 3.826 | 4.1634 | 4.875 | 4.0612 | 3.777 | 3.823 | 4.080 | 3.668 |
| ***(Gd/Yb)***$_N$ | 4.741 | 3.448 | 2.6631 | 4.399 | 3.8334 | 4.26 | 2.411 | 3.679 | 1.152 |
| ***La/Th*** | 3.327 | 3.186 | 2.8179 | 5.433 | 3.4954 | 3.219 | 2.575 | 3.436 | 3.191 |
| ***Th/U*** | 4.644 | 2.844 | 4.7097 | 6.983 | 5.6407 | 3.48 | 7 | 5.043 | 10.31 |
| ***Cr/Ni*** | 2.483 | 2.359 | 2.505 | 2.217 | 2.547 | 2.161 | 2.503 | 2.396 | 2.229 |
| ***V/Ni*** | 0.896 | 0.94 | 0.8438 | 0.993 | 0.6933 | 0.969 | 0.814 | 0.879 | 0.901 |
| ***Ni/Co*** | 4.899 | 4.738 | 4.2556 | 4.633 | 4.6669 | 4.934 | 4.455 | 4.654 | 4.806 |
| ***Cr/V*** | 2.771 | 2.51 | 2.9688 | 2.233 | 3.6739 | 2.229 | 3.073 | 2.780 | 2.474 |
| ***Rb/Sr*** | 0.262 | 0.477 | 0.382 | 0.232 | 0.881 | 0.392 | 0.426 | 0.436 | 1.392 |
| ***Nb/Ta*** | 9.869 | 6.861 | 11.338 | 11.591 | 15.366 | 10.121 | 8.071 | 10.460 | 18.232 |
| ***Zr/Hf*** | 33.36 | 33.35 | 34.58 | 33.65 | 34.75 | 34.32 | 34.10 | 34.02 | 33.47 |
| ***Th/Sc*** | 0.309 | 0.361 | 0.5238 | 0.343 | 0.2446 | 0.36 | 0.465 | 0.372 | 0.399 |
| ***La/Sc*** | 1.028 | 1.149 | 1.4761 | 1.862 | 0.8548 | 1.161 | 1.198 | 1.247 | 1.272 |
| ***Th/Ni*** | 0.038 | 0.047 | 0.0538 | 0.043 | 0.0305 | 0.044 | 0.048 | 0.044 | 0.054 |
| ***Th/Cr*** | 0.015 | 0.02 | 0.0215 | 0.019 | 0.012 | 0.021 | 0.019 | 0.018 | 0.024 |

Table. II. Continue……

| *Sample No.* | *BID-02* | *BID-05* | *BID-07* | *BID-09* | *B-06-07* | *Avg.* | *BHA-07* | *BHA-11* | *Avg.* |
|---|---|---|---|---|---|---|---|---|---|
| ***Sc*** | 40.7 | 32.087 | 65.578 | 15.37 | 42.064 | 39.159 | 32.63 | 41.193 | 36.912 |
| ***V*** | 296.3 | 283.15 | 436.26 | 131.77 | 323.808 | 294.255 | 236.96 | 250.15 | 243.553 |
| ***Cr*** | 203.2 | 402.47 | 747.22 | 358.06 | 185.297 | 379.258 | 240.71 | 518.78 | 379.742 |
| ***Co*** | 66.13 | 80.5 | 79.735 | 38.865 | 63.368 | 65.719 | 42.557 | 92.079 | 67.318 |
| ***Ni*** | 103.7 | 134.67 | 235.71 | 110.39 | 88.301 | 134.562 | 73.063 | 173.16 | 123.111 |
| ***Cu*** | 12.61 | 14.294 | 16.143 | 16.108 | 17.77 | 15.384 | 103.68 | 10.844 | 57.263 |
| ***Zn*** | 120.5 | 71.664 | 77.879 | 129.54 | 87.283 | 97.367 | 35.691 | 40.843 | 38.267 |
| ***Ga*** | 21.46 | 22.362 | 25.135 | 21.062 | 24.506 | 22.904 | 16.184 | 19.739 | 17.962 |
| ***Rb*** | 20.68 | 2.518 | 6.32 | 42.192 | 9.793 | 16.301 | 32.412 | 14.715 | 23.564 |
| ***Sr*** | 8.465 | 7.939 | 10.093 | 8.062 | 7.594 | 8.431 | 9.863 | 6.846 | 8.355 |
| ***Y*** | 31.11 | 16.469 | 8.542 | 12.026 | 25.202 | 18.669 | 28.707 | 18.674 | 23.691 |
| ***Zr*** | 134.2 | 165.78 | 30.75 | 125.61 | 201.954 | 131.662 | 237.49 | 130.7 | 184.097 |
| ***Nb*** | 7.845 | 6.662 | 5.184 | 8.744 | 9.976 | 7.682 | 10.052 | 1.038 | 5.545 |
| ***Cs*** | 4.912 | 1.248 | 0.944 | 0.894 | 1.081 | 1.816 | 0.962 | 19.851 | 10.407 |
| ***Ba*** | 31.66 | 10.475 | 17.437 | 58.58 | 16.614 | 26.953 | 77.885 | 35.313 | 56.599 |
| ***Hf*** | 3.642 | 4.522 | 1.056 | 3.836 | 5.548 | 3.721 | 6.676 | 3.683 | 5.180 |
| ***Ta*** | 0.656 | 0.5 | 0.44 | 0.516 | 1.151 | 0.653 | 0.813 | 0.236 | 0.525 |
| ***Pb*** | 9.128 | 8.897 | 8.886 | 11.219 | 10.557 | 9.737 | 22.566 | 16.791 | 19.679 |
| ***Th*** | 3.077 | 4.122 | 0.67 | 9.728 | 6.425 | 4.804 | 7.226 | 3.747 | 5.487 |
| ***U*** | 0.877 | 0.866 | 0.184 | 0.766 | 1.25 | 0.789 | 1.682 | 0.651 | 1.167 |
| ***La*** | 10.5 | 8.621 | 1.634 | 36.383 | 17.887 | 15.004 | 43.686 | 7.96 | 25.823 |
| ***Ce*** | 23.16 | 16.56 | 3.091 | 62.778 | 39.221 | 28.962 | 75.725 | 17.344 | 46.535 |
| ***Pr*** | 3.175 | 2.117 | 0.388 | 7.269 | 5.14 | 3.618 | 9.245 | 2.233 | 5.739 |
| ***Nd*** | 12.97 | 8.471 | 1.537 | 26.424 | 19.853 | 13.852 | 34.409 | 8.9 | 21.655 |
| ***Sm*** | 3.142 | 2.214 | 0.423 | 4.704 | 4.807 | 3.058 | 7.15 | 2.381 | 4.766 |
| ***Eu*** | 0.406 | 0.469 | 0.069 | 0.953 | 0.655 | 0.510 | 1.703 | 0.41 | 1.057 |
| ***Gd*** | 3.468 | 2.223 | 0.548 | 4.053 | 4.408 | 2.940 | 6.258 | 2.503 | 4.381 |
| ***Tb*** | 0.774 | 0.502 | 0.156 | 0.618 | 0.866 | 0.583 | 1.09 | 0.551 | 0.821 |
| ***Dy*** | 5.274 | 3.306 | 1.32 | 2.881 | 5.023 | 3.561 | 5.872 | 3.415 | 4.644 |
| ***Ho*** | 1.188 | 0.675 | 0.34 | 0.504 | 0.986 | 0.739 | 1.162 | 0.7 | 0.931 |
| ***Er*** | 3.556 | 1.951 | 1.26 | 1.332 | 2.796 | 2.179 | 3.405 | 2.104 | 2.755 |
| ***Tm*** | 0.636 | 0.347 | 0.269 | 0.189 | 0.516 | 0.391 | 0.625 | 0.37 | 0.498 |
| ***Yb*** | 3.863 | 2.115 | 1.951 | 1.14 | 3.219 | 2.458 | 3.871 | 2.213 | 3.042 |
| ***Lu*** | 0.662 | 0.35 | 0.363 | 0.196 | 0.56 | 0.426 | 0.676 | 0.383 | 0.530 |
| ***ΣREE*** | 72.78 | 49.921 | 13.349 | 149.42 | 105.937 | 78.281 | 194.88 | 51.467 | 123.172 |
| ***(La/Yb)$_N$*** | 1.836 | 2.754 | 0.566 | 21.566 | 3.755 | 6.096 | 7.626 | 2.431 | 5.028 |
| ***Eu/Eu**** | 0.376 | 0.646 | 0.438 | 0.667 | 0.43484 | 0.512 | 0.778 | 0.5132 | 0.646 |
| ***(La/Sm)$_N$*** | 2.103 | 2.451 | 2.431 | 4.868 | 2.342 | 2.839 | 3.8458 | 2.1043 | 2.975 |
| ***(Gd/Yb)$_N$*** | 0.728 | 0.852 | 0.228 | 2.881 | 1.11 | 1.160 | 1.3102 | 0.9167 | 1.113 |
| ***La/Th*** | 3.411 | 2.0915 | 2.4388 | 3.74 | 2.78397 | 2.893 | 6.0457 | 2.1244 | 4.085 |
| ***Th/U*** | 3.509 | 4.7598 | 3.6413 | 12.7 | 5.14 | 5.950 | 4.2961 | 5.7558 | 5.026 |
| ***Cr/Ni*** | 1.959 | 2.9886 | 3.1701 | 3.2437 | 2.09847 | 2.692 | 3.2945 | 2.996 | 3.145 |
| ***V/Ni*** | 2.856 | 2.1026 | 1.8508 | 1.1937 | 3.66709 | 2.334 | 3.2432 | 1.4446 | 2.344 |
| ***Ni/Co*** | 1.569 | 1.6729 | 2.9562 | 2.8403 | 1.39346 | 2.086 | 1.7168 | 1.8805 | 1.799 |
| ***Cr/V*** | 0.686 | 1.4214 | 1.7128 | 2.7173 | 0.57224 | 1.422 | 1.0158 | 2.0739 | 1.545 |
| ***Rb/Sr*** | 2.443 | 0.317 | 0.626 | 5.233 | 1.290 | 1.982 | 3.286 | 2.149 | 2.718 |
| ***Nb/Ta*** | 11.959 | 13.324 | 11.782 | 16.946 | 8.667 | 12.536 | 12.364 | 4.398 | 8.381 |
| ***Zr/Hf*** | 36.85 | 36.66 | 29.12 | 32.75 | 36.40 | 34.36 | 35.57 | 35.49 | 35.53 |
| ***Th/Sc*** | 0.076 | 0.1285 | 0.0102 | 0.6329 | 0.15274 | 0.200 | 0.2215 | 0.091 | 0.156 |
| ***La/Sc*** | 0.258 | 0.2687 | 0.0249 | 2.3671 | 0.42523 | 0.669 | 1.3388 | 0.1932 | 0.766 |
| ***Th/Ni*** | 0.03 | 0.0306 | 0.0028 | 0.0881 | 0.07276 | 0.045 | 0.0989 | 0.0216 | 0.060 |
| ***Th/Cr*** | 0.015 | 0.0102 | 0.0009 | 0.0272 | 0.03467 | 0.018 | 0.03 | 0.0072 | 0.019 |

Clay minerals probably were the initial hosts for the LILE elements as indicated by correlations between Rb, Ba and $K_2O$ (Fig. 16). Ba displays the largest scatter when plotted against Zr, corresponding to stronger post depositional element mobility (Fig. 17). In contrast, U and Th behave extremely coherently as witnessed by the strong linear trend in Th-U space (Fig. 18), corresponding to an average Th/U ratios of 5.04 (Pavagada), 5.95 (Bidaloti) and 5.03 (Bandihalli), slightly higher than in chondrites (4.2, Kramers and Tolstikhin, 1997), while, Duntur pelite show higher Th/U ratio (10.31) which may be due to intense fluid activity mainly $CO_2$ fluid front (Janardhan et al. 1990) that flush out U as Duntur area is in granulite transition zone.

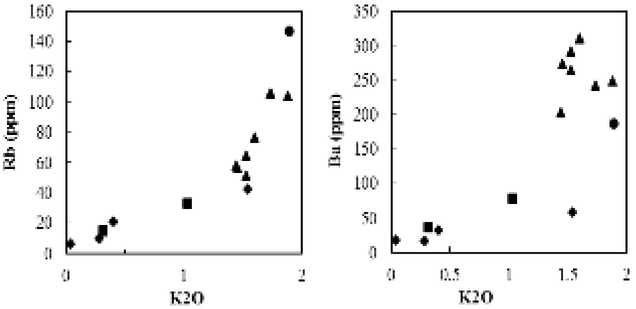

Fig. 16. Plots showing correlation between Rb, Ba and $K_2O$.

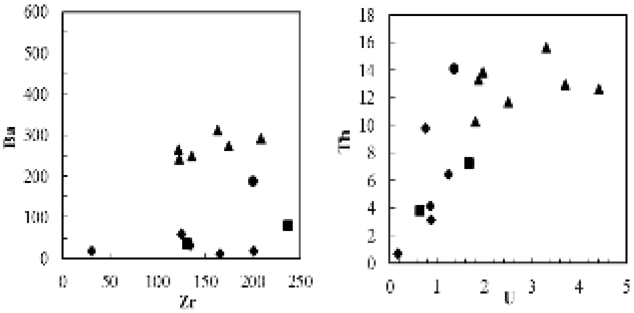

Fig. 17 & 18. Zr v/s Ba and Th v/s U plots

Strontium concentrations are notably low in metapelites of Bidaloti and Bandihalli area, and Rb/Sr ratios are high. Whereas Pavagada and Duntur metapelites shows much higher Sr and low Rb/Sr ratios as similar to metasediments from most Archaean sedimentary sequences (Mass and McCulloch 1991). High Rb/Sr could either reflect the source composition or may be due to intense source rock weathering and/or strong mineral control (e.g., mixing of mica and quartz) (Mass and McCulloch 1991).

Average Th values in metapelites from Pavagada (12.86ppm) and Duntur (14.07 ppm) are similar or higher than the levels found in other Archaean fine-grained sediments (5-10 ppm, Taylor and McLennan, 1985). Such high Th levels are also observed in other mid-Archaean cratonic sedimentary sequences such as Pongola Supergroup (group means of up to 13 ppm, Wronkiewicz and Condie, 1989) and the K-8 shales from the upper Witwatersrand supergroup (10ppm, Wronkiewicz and Condie, 1987). Dominantly K-rich granitic sources have been inferred for Pongola and K-8 shales. The high Th in Pavagada and Duntur area has been probably introduced during migmatization and injection of Closepet granite type veins and also may be due to the presence of felsic plutonic components in the source in small quantities (about 5%) (Taylor and McLennan 1985).

Average Th in metapelites from Bidaloti (4.80 ppm) and Bandihalli (5.49 ppm) is similar or lower than the levels found in other Archaean fine-grained sediments (5-10 ppm, Taylor and McLennan, 1985) and much lower abundances than typical of post-Archaean sediments (PAAS 14.6 ppm, Taylor and McLennan 1985; NASC 12 ppm).

### *High Field Strength Elements (HFSE):*

The elements Zr, Nb, Hf, Ta, Y, Th and U are preferentially partitioned into melts during crystallization and anatexis (Feng and Kerrich, 1990), and as a result, these elements are enriched in felsic rocks rather than mafic ones. Additionally, along with the REE's, these high field strength elements are immobile and thought to reflect provenance compositions (Taylor and McLennan, 1985).

Studied metapelites show local variations in the distribution of HFSE (Y, Zr, Nb, Hf and Ta). Pairs of Zr-Hf and Nb-Ta form well-defined linear correlations (Fig. 19 & 20) corresponding to Nb/Ta average values 10.46 (Pavagada), 12.54 (Bidaloti), 8.38 (Bandihalli), 18.23 (Duntur) and Zr/Hf average values 34.02 (Pavagada), 34.36 (Bidaloti), 35.53 (Bandihalli), 33.47 (Duntur), slightly similar to those for NASC, (Nb/Ta=11.6, Zr/Hf=31.7). The wide range in concentrations documents contributions from compositionally variable source rocks. Well-defined linear trends with zero-intercepts render secondary fractionation processes are negligible.

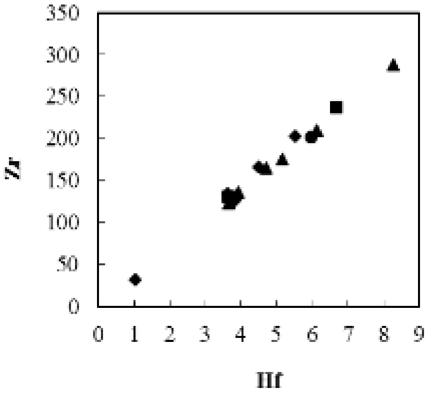

Fig. 19. Hf v/s Zr plot for studied metapelites.

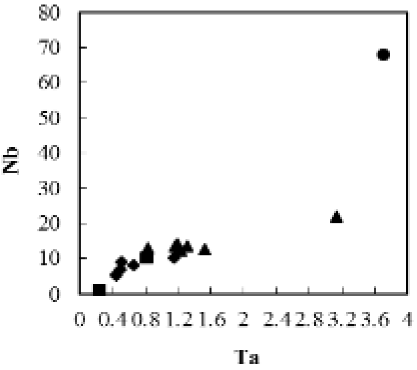

Fig. 20. Ta v/s Nb plots for studied metapelites

***Transition metals:***

Feng and Kerrich (1990) noted that Cr, Co, Ni and Ti-V may be fractionated during weathering. The studied samples from Pavagada and Duntur areas show high Cr and Ni abundances with Cr vary from 582 – 853 ppm and Ni from 261 – 335 ppm. Co varies from 54 – 72 ppm, V from 223 – 319 ppm, this also result in anomalously high Ni/Co (4.3 – 4.9), Cr/V (2.2 – 3.7), Cr/Ni (2.2 – 2.5) and low V/Ni (0.7 – 1.0). When compared with the crustal abundances (Shaw, 1980), NASC (Gromet et al., 1984) and PAAS (Taylor and McLennan 1985), the Ni, Co, Cr and V of metapelites of the Pavagada and Duntur areas are relatively higher. Cr/V ratios for the Pavagada and Duntur metapelites (2.2 – 3.7) are intermediate between those of early (5.3) and late-Archaean (1.5) shales (Taylor and McLennan, 1985) but well above the post-Archaean shales (<1); Ni/Co ratios show an analogous relationship. This suggests mixed source lithologies with more contributions from ultramafic/mafic rocks to the Pavagada and Duntur metapelites were significant. The large variation in Cr/V and Ni/Co would further suggest variable degrees of chemical weathering of the ultramafic/mafic source rocks which would tend to selectively enrich weathering products in Cr and Ni (Wronkiewicz and Condie, 1989; Taylor and McLennan, 1985).

Bidaloti and Bandihalli metapelites (except BID-07) show moderate Cr and Ni abundances when compared to Pavagada and Duntur metapelites. The Cr values from 185 – 519 ppm and Ni from 73 – 173 ppm. Co varies from 39-92 ppm, V from 132- 436 ppm. Elemental ratios, Ni/Co varies from 1.39-2.96, Cr/V from 0.57-2.72, Cr/Ni from 1.96-3.29, and V/Ni from 1.19-3.67. Cr/V ratio of the samples BID-09 and BHA-11 are intermediate between those of early (5.3) and late-Archaean (1.5) shales (Taylor and McLennan, 1985) but well above the post-Archaean shales (<1), whereas Cr/V ratios of samples BID-02, B-06-07 and BHA-07 are similar to post-Archaean shales (<1). Though the Co, Cr, Ni and V values of these areas are relatively lower than other studied areas, they compare well with the late Archaean shales and reflect the same source conditions of the others, but with slight difference in mafic/felsic proportions in the source regions. Covariations between transition metals (Co, Ni, Cr) and MgO, $Fe_2O_3$ are lacking (Fig. 21). In contrast, strong covariations were found for Co-Ni, Co-Cr and Co-V (Fig. 22). The strongest correlation exists between Cr and Ni (Fig. 23).

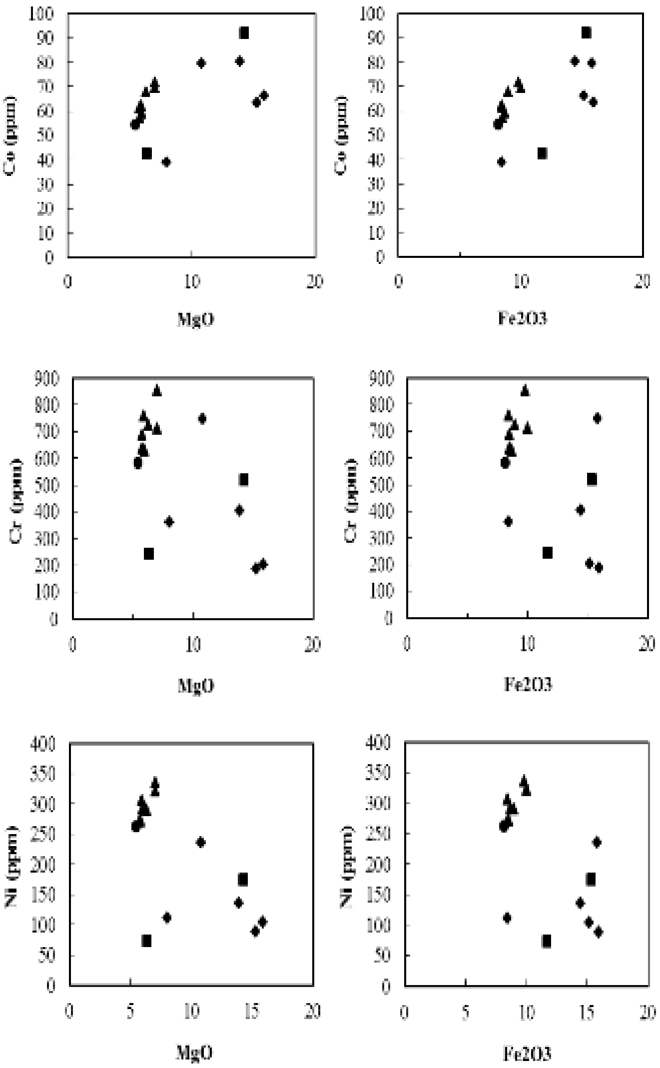

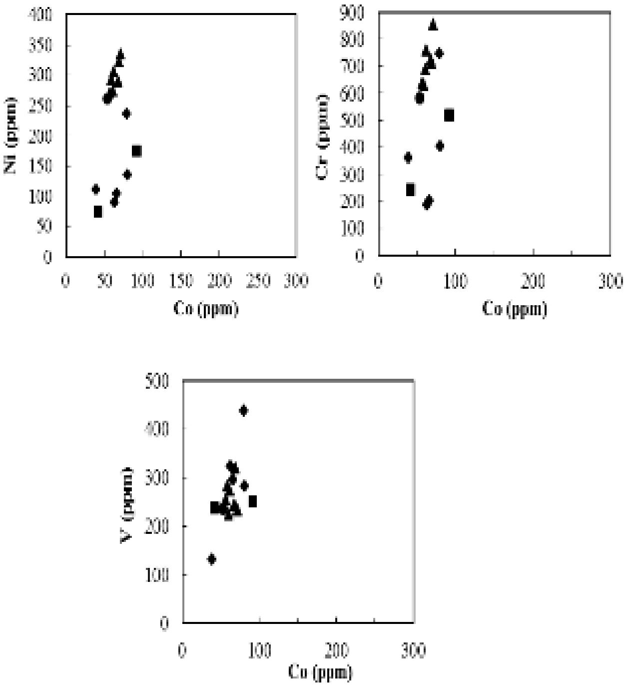

Fig. 22. Transition elements v/s Co plot.

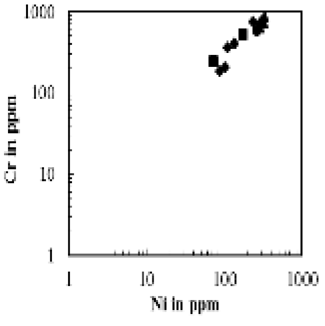

Fig. 21. Transition elements v/s MgO and $Fe_2O_3$ plots.

Fig. 23. Ni v/s Cr plot.

### *Rare Earth Elements (REE):*

Rare Earth Elements (REE) are relatively insoluble elements, with short residence times in the ocean (Taylor and McLennan 1985). Accordingly, they are transferred almost quantitatively from upper crustal sources to terrigenous sedimentary rocks. The observed uniformity of REE patterns in post-Archaean terrigenous sedimentary rocks, in contrast to the diversity of source rock patterns, is interpreted to indicate that the processes of erosion, transportation and deposition provide through mixing and averaging of these differing source patterns. Thus the REE patterns preserved in the sedimentary record provide an overall average of the composition of the upper crustal rocks exposed to erosion and find important applications in sedimentary rocks particularly understanding the provenance. REE patterns of detrital sediments reflect their source.

Chondrite values of Taylor and McLennan (1985) are used for normalizing the REE values of the studied metapelites and the REE patterns are shown in Fig. 24. Metapelites of Pavagada area show higher total REE (149-306), ($(La/Yb)_{N=}$ 14.43-34.80) abundances and are characterized by LREE enrichment ($(La/Sm)_{N=}$ 3.8-4.9) and HREE depletion ($(Gd/Yb)_N$=2.4-4.74). All the analyzed pelites show no Eu anomaly (Eu/Eu*= 0.83-1.07) except for one sample (P-15) which shows slight negative Eu anomaly (Eu/Eu*= 0.72).

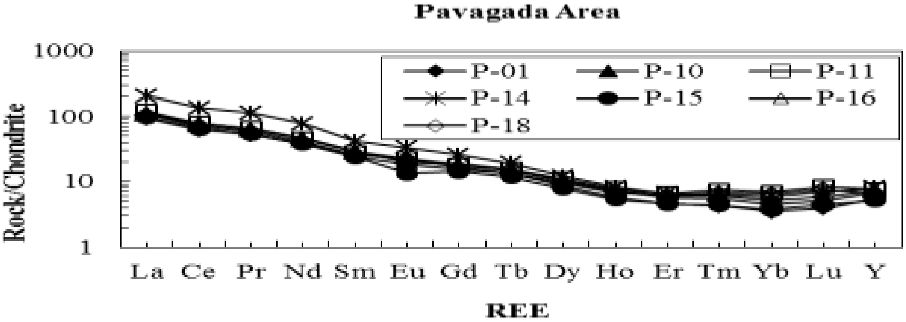

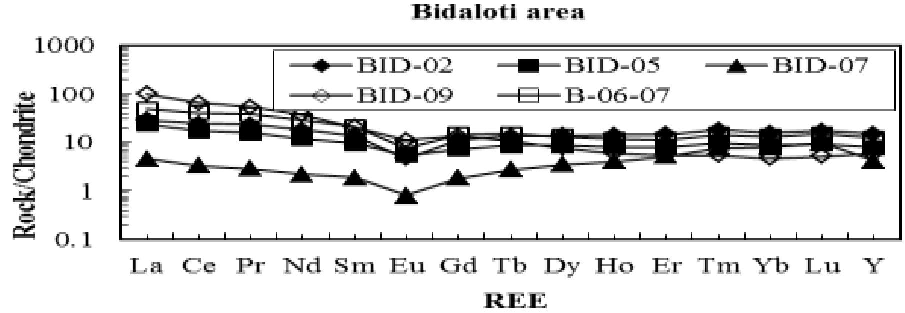

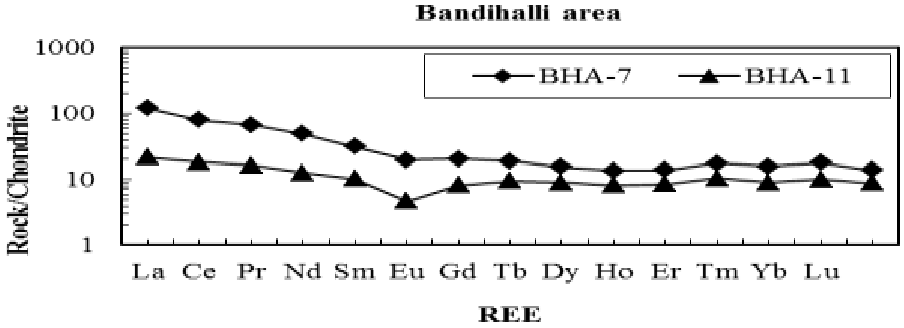

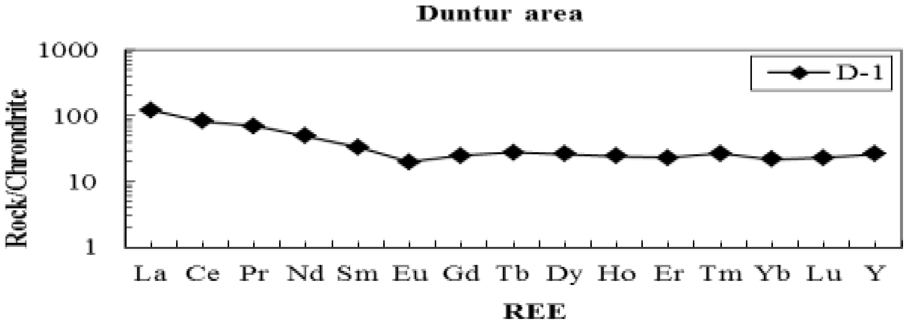

Fig. 24. REE patterns of studied metapelites.

The general lack of Eu-depletion in sediments is attributed to the presence of intracrustal igneous rocks with negative Eu anomaly as minor components in the provenance (Taylor and McLennan 1985). Since the metapelites of Pavagada area show lack of significant Eu depletion may indicate the presence of mafic igneous rocks in the provenance which were not involved in crustal melting, which is further attested by high Cr and Ni (see Table. II).

Presence of high values of Cr, Ni can only be explained by the presence of ultramafic/mafic rock in the source region. Though the REE pattern and abundances of other incompatible elements do not reflect the same. This anomaly can be explained only by visualizing a mixture of rocks (both mafic and felsic rocks (volcanic/plutonic)) in the provenance. The over all REE abundance like LREE enrichment and no Eu depletion are comparable to Archaean sedimentary rocks.

Metapelites of Bidaloti area are characterized by LREE enrichment ($(La/Sm)_{N=}$ 2.1-4.87), flat HREE ($(Gd/Yb)_N$=0.22-2.88), and pronounced negative Eu-anomalies (Eu/Eu* = 0.38-0.67) with low to medium total REE (13.35-149.42) and $(La/Yb)_{N=}$0.56-21.57.

The overall REE pattern and significant negative Eu anomalies compare very well with average post-archaean shales (PAAS; Nance and Taylor, 1976) than to Archaean sedimentary rocks. Further REE and moderate Cr, Ni in these metapelites reflect a mixed source with preponderance of felsic rocks.

Metapelites of Bandihalli area are characterized by LREE ($(La/Sm)_{N=}$2.1-3.8) enrichment, flat HREE ($(Gd/Yb)_N$=0.92-1.3) and negative Eu-anomalies (Eu/Eu* = 0.51 – 0.78) with medium to high total REE (51.47-194.88) and $(La/Yb)_{N=}$2.43-7.63.

The over all REE pattern and significant negative Eu anomalies compares very well with average post-archaean shales (PAAS; Nance and Taylor, 1976) than to archaean sedimentary rocks. Further REE and moderate Cr, Ni in these metapelites reflect a mixed source with preponderance of felsic rocks.

The REE pattern of the Duntur area metapelite show higher total REE (213.01), $(La/Yb)_N$=5.66 abundance and characterized by LREE enrichment ($(La/Sm)_{N=}$3.67), flat HREE ($(Gd/Yb)_N$=1.15). The studied metapelites shows pronounced negative Eu-anomaly (Eu/Eu* =0.69).

The over all REE pattern and significant negative Eu anomalies compare very well with average post-archaean shales (PAAS; Nance and Taylor, 1976) than to Archaean sedimentary rocks. Further REE and higher Cr, Ni in these metapelite reflect a mixed source (both mafic and felsic rocks (volcanic/plutonic) for the provenance.

## IV ISOTOPE DATA

In the present study whole rock Rb-Sr and Sm-Nd isotope analysis for representative samples of metapelites was carried out and the data is presented in Table III & IV. Several samples show anomalous Rb/Sr (i.e. $^{87}Rb/^{86}Sr$) values and also intial 87Sr/86Sr values. This could be probably related to alteration of Rb/Sr ratios during metamorphism, where the associated fluid flow either removed or introduced Rb. There is growing evidence of 3.0 Ga thermal event (Jayananda et al 2011), 2.62 Ga metamorphic event (Chitradurga granite) and last 2.52 Ga major thermal event (Closepet type granite intrusives) in the Eastern Dharwar craton. Once Rb/Sr ratios are altered which affect $^{87}Rb/^{86}Sr$ ratios which results in anomalous values. Consequently the observed anomalous $^{87}Rb/^{86}Sr$ values do not provide any precise information on provenance, but reflect Rb mobility during metamorphism, fluid flow or contemporaneous magmatic accretion.

Table. III. Whole rock Rb-Sr isotopic data of studied metapelites.

| Sample | Rb ppm | Sr ppm | $^{87}Rb/^{86}Sr$ | Err. in X | $^{87}Sr/^{86}Sr$ | Error in Y | Lambda L*t | Exp(Lt)-1 | ($^{87}Rb/^{86}Sr$)*(Exp(Lt)-1) | $(^{87}Sr/^{86}Sr)_i$ |
|---|---|---|---|---|---|---|---|---|---|---|
| P-01 | 37.309 | 159.192 | 0.6805 | | 0.743468 | 0.000080 | 0.042600 | 0.043520 | 0.029616 | 0.713852 |
| P-10 | 53.637 | 130.923 | 1.1918 | | 0.761666 | 0.000060 | 0.042600 | 0.043520 | 0.051868 | 0.709798 |
| P-11 | 17.608 | 182.996 | 0.2798 | | 0.758391 | 0.000020 | 0.042600 | 0.043520 | 0.012177 | 0.746214 |
| P-14 | 23.745 | 147.322 | 0.4655 | | 0.691801 | 0.000030 | 0.042600 | 0.043520 | 0.020259 | 0.671542 |
| P-15 | 39.081 | 4.610 | 2.4912 | | 0.826993 | 0.000060 | 0.042600 | 0.043520 | 0.108418 | 0.718575 |
| P-16 | 43.851 | 125.868 | 1.0117 | | 0.746692 | 0.000060 | 0.042600 | 0.043520 | 0.044030 | 0.702662 |
| P-18 | 28.404 | 85.997 | 0.9601 | | 0.760999 | 0.000010 | 0.042600 | 0.043520 | 0.041784 | 0.719215 |
| BID-02 | 23.185 | 3.350 | 21.1806 | | 1.668478 | 0.000030 | 0.042600 | 0.043520 | 0.921788 | 0.746690 |
| BID-09 | 19.852 | 2.331 | 27.0458 | | 1.935759 | 0.000010 | 0.042600 | 0.043520 | 1.177044 | 0.758715 |
| B-06-7 | 7.009 | 2.865 | 7.1531 | | 0.949489 | 0.000030 | 0.042600 | 0.043520 | 0.311306 | 0.638183 |
| BHA-7 | 17.807 | 3.487 | 15.7054 | | 1.436985 | 0.000030 | 0.042600 | 0.043520 | 0.683505 | 0.753480 |
| BHA11 | 11.119 | 2.196 | 15.4250 | | 1.202650 | 0.000002 | 0.042600 | 0.043520 | 0.671302 | 0.531348 |
| D-1 | 103.068 | 77.282 | 3.9150 | | 0.861607 | 0.000042 | 0.042600 | 0.043520 | 0.170382 | 0.691225 |

Table. IV. Whole rock Sm-Nd isotopic data of studied metapelites.

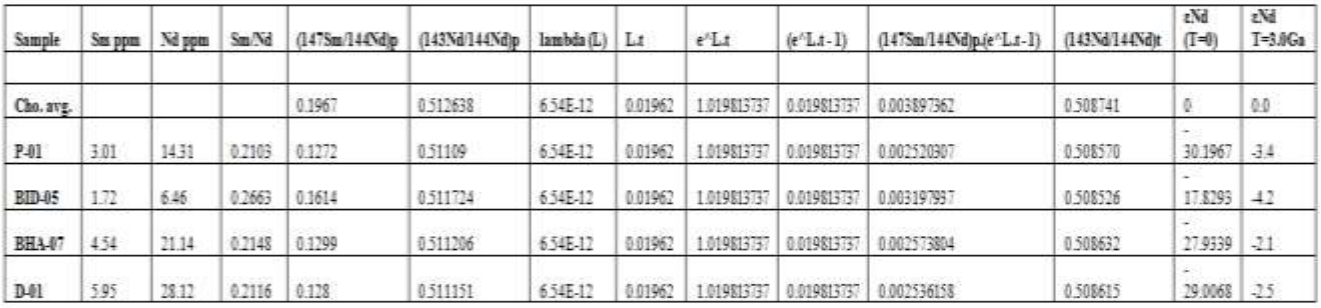

| Sample | Sm ppm | Nd ppm | Sm/Nd | (147Sm/144Nd)p | (143Nd/144Nd)p | lambda (L) | L.t | e^L.t | (e^L.t-1) | (147Sm/144Nd)p.(e^L.t-1) | (143Nd/144Nd)t | εNd (T=0) | εNd T=3.0Ga |
|---|---|---|---|---|---|---|---|---|---|---|---|---|---|
| | | | | | | | | | | | | | |
| Cho. avg. | | | | 0.1967 | 0.512638 | 6.54E-12 | 0.01962 | 1.019813737 | 0.019813737 | 0.003897362 | 0.508741 | 0 | 0.0 |
| P-01 | 3.01 | 14.31 | 0.2103 | 0.1272 | 0.51109 | 6.54E-12 | 0.01962 | 1.019813737 | 0.019813737 | 0.002520307 | 0.508570 | -30.1967 | -3.4 |
| BID-05 | 1.72 | 6.46 | 0.2663 | 0.1614 | 0.511724 | 6.54E-12 | 0.01962 | 1.019813737 | 0.019813737 | 0.003197937 | 0.508526 | -17.8293 | -4.2 |
| BHA-07 | 4.54 | 21.14 | 0.2148 | 0.1299 | 0.511206 | 6.54E-12 | 0.01962 | 1.019813737 | 0.019813737 | 0.002573804 | 0.508632 | -27.9339 | -2.1 |
| D-01 | 5.95 | 28.12 | 0.2116 | 0.128 | 0.511151 | 6.54E-12 | 0.01962 | 1.019813737 | 0.019813737 | 0.002536158 | 0.508615 | -29.0068 | -2.5 |

On the other hand Sm-Nd isotope system is more robust as Nd is less mobile. Thus Sm-Nd system can be used to evaluate the history of provenance. Sm-Nd isotope data is presented in Table. IV indicate Sm/Nd ratios, $^{143}Nd/^{144}Nd$, Nd model ages and εNd (at 3.0Ga) values are not affected by anomalous Sm/Nd ratios and they are more realistic, which can be used to evaluate source (provenance) history.

Several samples show anomalous Nd model ages(either too high or too low) this is probably related to anomalous Sm/Nd ratios developed during metamorphism due to growth of minerals like garnet (high Sm/Nd). Sm-Nd isotope data is used to calculate Nd model ages and εNd values to characterize timing of accretionary processes and petrogenetic mechanisms including source reservoirs.

The metapelites from Pavagada area defines negative ε Nd values (-3.4) at 3000 Ma with $T_{DM}$ Nd model age of 3560 Ma (see Table. V) using depleted mantle model, which corresponds to εNd (T=3000 Ma) values. Similarly, Bidaloti area metapelite also defines negative εNd value (-4.2) at 3000 Ma with $T_{DM}$ Nd model age of 3600 Ma (see Table. V). Such values indicate that the provenance of Pavagada and Bidaloti has extended crustal history prior to 3.0 Ga, possibly sources differentiated from depleted mantle during 3.5-3.6Ga.

Table. V. Whole rock Sm-Nd isotopic data of studied metapelites.

| Area | Sample ID | Nd ppm | Sm ppm | $^{147}Sm/^{144}Nd$ | $^{143}Nd/^{144}Nd$ | Error Y | $T_{DM}$ Ga |
|---|---|---|---|---|---|---|---|
| ***Pavagada*** | P-01 | 14.31 | 3.01 | 0.1272 | 0.51109 | 0.000002 | 3.56 |
| ***Bidaloti*** | BID-09 | 11.71 | 2.35 | 0.1213 | 0.510773 | 0.000005 | 3.6 |
| ***Bandihalli*** | BHA-07 | 21.14 | 4.54 | 0.1299 | 0.511206 | 0.000007 | 3.47 |
| ***Duntur*** | D-01 | 28.12 | 5.95 | 0.128 | 0.511151 | 0.000001 | 3.49 |

Metapelite from Bandihalli area defines negative εNd value (-2.1) at 3000 Ma with $T_{DM}$ Nd model age of 3470 Ma (see Table. V) using depleted mantle model, which corresponds to ε Nd (T=3000 Ma) values. Similarly, Duntur area metapelite also defines negative εNd value (-2.5) at 3000 Ma with $T_{DM}$ Nd model age of 3490 Ma (see Table. V). The Nd isotopic data indicate provenance of Bandihalli and Duntur have shorter crustal history prior to 3.0Ga, probably differentiated from depleted mantle during 3.3-3.4Ga.

## V DISCUSSION AND CONCLUSION

The outcomes of geochemistry and isotopic studies of the metapelites to characterize Paleoweathering, tectonic settings and also to delineate sediment source and finally to trace the Archaean crustal evolution in the Eastern Dharwar craton is discucessed in the following paragraphs.

### Paleoweathering conditions:

Chemical weathering has important effects on the composition of siliciclastic rocks, where larger cations (e.g. Rb, Ba), remain fixed in the weathered residue, in preference to smaller cations (Na, Ca, Sr) which are selectively leached (Nesbitt et al., 1980). These chemical trends may be transferred to the sedimentary record (Nesbitt and Young, 1982; Wronkiewicz and Condie, 1987), and thus provide a useful tool for monitoring source area. The enrichment of immobile elements like $SiO_2$, $Al_2O_3$, $TiO_2$, Rb and Ba and depletion of $Na_2O$, CaO and Sr in the studied samples suggests strong chemical weathering. Further Nesbitt and Young (1982) defined a chemical index of alteration (CIA) to quantitatively measure the degree of weathering. It is calculated using the molecular proportions of major oxides as indicated in the equation CIA= $[(Al_2O_3/(Al_2O_3+CaO^*+Na_2O+K_2O)] \times 100$. CIA values for average shales range from 70-75 (of a possible 100) and sometimes the value reaches 100 which indicates intense weathering. CIA values of studied metapelites of Pavagada range from 70 – 89, Bidaloti from 82 – 94, Bandihalli from 84 – 86 and a single metapelite sample from Duntur has a CIA value of 82, these values are high when compared to that of NASC ((CIA= avg 57.12) and PAAS (CIA= avg 70) (Taylor and McLennan, 1985)). Thus, the CIA values of the studied metapelites suggest moderate to intense chemical weathering of the source rocks. Further the calculated PIA (i.e. PIA= $[(Al_2O_3-K_2O)/(Al_2O_3+CaO^*+Na_2O-K_2O)] \times 100$, Fedo et al., 1995) values of the metapelites of the Pavagada (82.35), Bidaloti

(90.57), Bandihalli (89.50) and Duntur (87.18) areas not only indicates the same weathering condition but also near alteration of plagioclase. Such an inference is also supported by the average weathering trend of the studied metapelites on A-CN-K diagram (where A, CN and K refers to $Al_2O_3$, $CaO+Na_2O$ and $K_2O$ respectively) which corresponds to smectite, gibbsite, chlorite and kaolinite end members (Fig. 25).

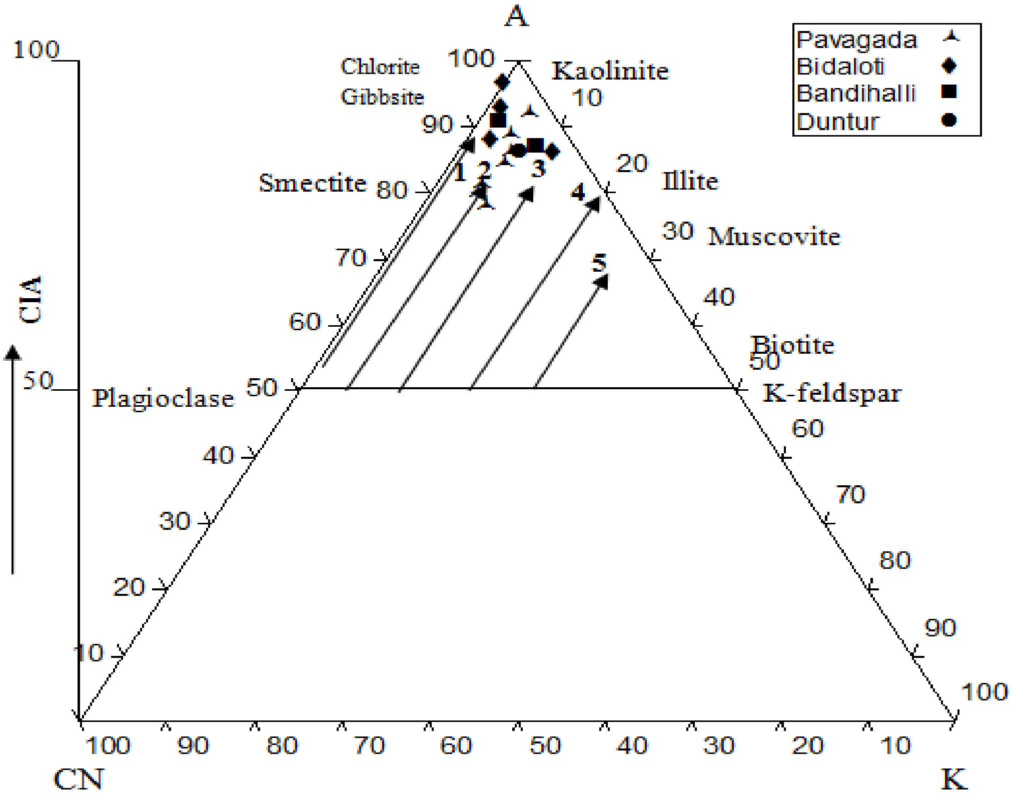

Fig. 25. Al2O3 - CaO*+Na2O - K2O (A-CN-K) ternary diagram (Nesbitt and Young, 1982). Numbers 1-5 denote compositional trends of initial weathering profiles of different rocks: 1- Gabbro; 2-tonalite; 3-diorite; 4-granodiorite; 5-granite.

**Source rock composition:**

Useful elements for defining the composition of a sediment source area are those which are least mobile during weathering, transport and diagenetic metamorphic processes, such as the REE, Th, Sc and the HFSE (Taylor and McLennan, 1985). Cr/Th and Th/Sc ratios are also useful as indicators for the bulk composition of the provenance (Wronkiewicz and Condie, 1987; Condie and Wronkiewicz, 1990).

Nickel and chromium serve as provenance indicators in sedimentary rocks where ultramafic sources are suspected (Taylor and McLennan, 1985; Condie and Wronkiewicz, 1990; Garver et al., 1996; Young and Nesbitt, 1999), with consideration that chromium may be mobilized by secondary processes and therefore limited in some cases as a provenance indicator (Nagender Nath et al., 2000).

Thorium and scandium are marker elements for felsic and mafic igneous rocks, respectively. REE have long been considered appropriate provenance indicators, due to their short residence times in solution and an apparent tendency to be transferred almost completely from weathering profiles and parent rocks to the clastic sedimentary system, particularly shales (Nesbitt, 1979; Cullers et al., 1987; Cullers, 1988; McLennan, 1989; Nesbitt and Markovics, 1997).

Generally it is believed that post-Archaean pelites have less concentration of mafic elements, particularly Ni and Cr, compared with the Archaean pelites. The cause of higher concentrations in Archaean pelites has been explained by the presence of an ultramafic/mafic component in the Archaean source, whereas scarcity of ultramafic/mafic component in the post-Archaean have been invoked for the low content of Ni and Cr in the post-Archaean pelites (McLennan et al., 1983). On the Ni-Cr diagram (Fig. 26) Pavagada and Duntur area metapelites plot within the early Archaean field, where as Bidaloti and Bandihalli area metapelites plot within the late Archaean field. The observed trace element data of studied metapelites reflect the presence of ultramafic/mafic rocks in the provenance. Further, Th/Sc ratios are less than one (Pavagada= 0.24-0.52, Bidaloti=0.07-0.63, Bandihalli=0.09-0.22 and Duntur=0.39) for the studied metapelites also indicate a contribution of ultramafic/mafic source.

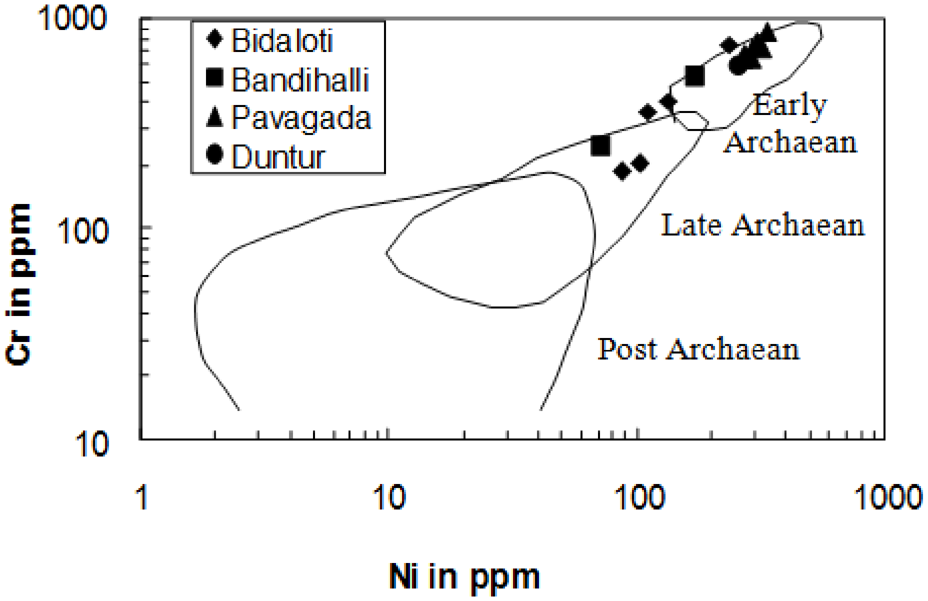

Fig. 26. Ni Vs Cr diagram, Pelite fields after Taylor and McLennan (1985).

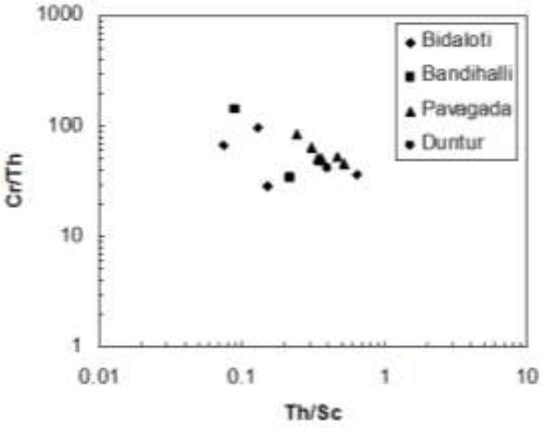

Fig. 27. Cr/Th versus Th/Sc diagram after Taylor and McLennan 1985.

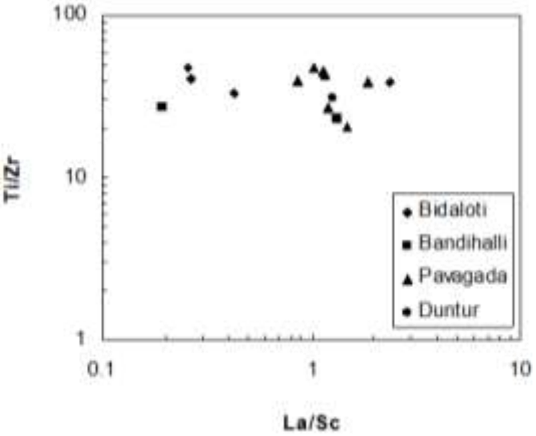

Fig. 28. Ti/Zr versus La/Sc diagram after Taylor and McLennan 1985

Pavagada and Duntur area metapelites were relatively similar in their major element chemistry and indicate their derivation from similar source. However, $Al_2O_3$ content (18.96-25.19wt %, except P-18) of these metapelites is high which may be due to high volume % of Sillimanite. Whereas metapelites from Bidaloti and Bandihalli area were similar and derived from mafic rich source as indicated by their MgO and $Fe_2O_3$ content (average MgO content varies from 10.38-12.88wt% and $Fe_2O_3$ from 13.56-14wt %).

The A-CN-K triangle can also be used to constrain initial compositions of source rocks and to examine their weathering trends because the upper crust is dominated by plagioclase and K-feldspar rich rocks and their weathering products (Fedo et al., 1995; Nesbitt and Young, 1984, 1989). Many weathering profiles show a linear trend subparallel to A-CN join in the A-CN-K triangle (Nesbitt and Young, 1984). In the absence of K-metasomatism, a line extends through the data points intersects the feldspar join at a point that shows the proportion of plagioclase and K-feldspar of the fresh rock. This proportion yields a good indication of the type of the parent rock. A metasomatised sample suite will typically have a linear trend with a less steep slope, because the amount of K-addition but its intersection with the feldspar join indicates the likely source rock composition (Fedo et al., 1995). The studied samples do not show any linear trend parallel or subparallel to A-CN join except for the Pavagada samples which plot along tonalite trend (Fig. 25). Other samples show wide scatter on the A-CN-K plot, their value plot between diorite and tonalite.

The relative contribution of mafic and felsic sources in the pelites should be reflected in the distribution of Zr and Cr in pelites (Wronkiewicz and Condie, 1989). The studied metapelites are enriched in both Zr and Cr (see Table. 2), thus it may indicate mixed nature of provenance.

Finally based on major elements, LILE, HFSE, Transition element contents, Rb/Sr, Th/U, Zr/Y, Th/Sc, Nb/Ta, Zr/Hf, Cr/Ni, Ni/Co, Cr/Y, Eu/Eu* ratios and REE patterns of the studied metapelites from the Eastern Dharwar Craton indicates heterogeneous sources involving varying proportions of ulramfaic-mafic and felsic TTG sources.

**Tectonic setting:**

The chemical approach is a useful complement to petrographic analysis, and the two methods when combined, become a powerful tool for examination of provenance and determination of tectonic setting. Sedimentologists and geochemists have long endeavored to pursue the relationship between sedimentary rock geochemistry and plate tectonics for recognizing ancient tectonic settings (Armstrong-Altrin and Verma, 2005; Bhatia and Taylor, 1981; Bhatia, 1983, 1985a, b; Bhatia and Crook, 1986; Crook, 1974; Floyd et al., 1991; Gu, 1994; Gu et al., 2002; Maynard et al., 1982; McLennan et al., 1990; Middleton, 1960; Roser and Korsch, 1985, 1986, 1988; Schwab, 1975). Studies in the last decade have shown some complications when composition is related to tectonic setting (Cullers, 1988; McLennan et al., 1990), but such an effort does give insight to the ways in which tectonics and the geochemical processes interact in determining the compositions of sediments.

Some authors have described the usefulness of major elements geochemistry of sedimentary rocks to infer tectonic setting based on discrimination diagrams (Bhatia, 1983; Roser and Korsch, 1986), although others have pointed out the difficulties in using geochemistry to interpret tectonic setting (Armstong-Altrin and Verma, 2005; Silodowski and Zalasiewicz, 1991; Nesbitt and Young, 1989; Van de Kamp and Leake, 1985). The geochemistry of sedimentary rocks is a complex function of the nature of source rocks, intensity and duration of weathering, sedimentary recycling, diagenesis and sorting (Argast and Donnelly, 1986; Cullers, 2000; McLennan et al., 1993). Furthermore, specific tectonic settings do not necessarily produce rocks with unique geochemical signatures (Banlburg, 1998; McLennan et al., 1990). In some instances, sediments are transported from one tectonic setting into a sedimentary basin having different tectonic environment (McLennan et al., 1990). Inspite of these difficulties, the geochemistry of sedimentary rocks have been used to infer the tectonic setting of ancient sedimentary basins (Burnett and Quirk, 2001; Gu et al., 2002; Kasper-Zubillega et al., 1999).

Based on nature of Archaean crust, Bhatia (1983) divided continental margins and oceanic basins into four tectonic settings viz. oceanic island arcs (OIA), continental island arc (CIA), active continental margin (ACM) and passive continental margin (PM). He proposed that the most discriminating parameters to decipher different tectonic settings are $Fe_2O_3$+MgO, $TiO_2$, and $Al_2O_3/SiO_2$, $K_2O/Na_2O$ and $Al_2O_3/(CaO+Na_2O)$ as shown in Table. VI. The geochemical concept behind the discrimination parameters was based on general decrease in $Fe_2O_3$+MgO, $TiO_2$ and $Al_2O_3/SiO_2$ and an increase in $K_2O/Na_2O$ and $Al_2O_3/(CaO+Na_2O)$ as the tectonic setting changes in the sequence OIA →CIA→ACM→PM.

It is evident from the Table. VI that $Fe_2O_3$+MgO (wt%), $TiO_2$ (wt%), $Al_2O_3/SiO_2$ values of the studied samples are comparable with that of oceanic island arc (OIA) of Bhatia (1983), whereas $KO/Na_2O$ and $Al_2O_3/(CaO+Na_2O)$ values are comparable with that of passive margin setting (PM) of Bhatia (1983).

Table. VI. Tectonic geochemical discriminating parameters (Bhatia, 1983) compared with the studied metapelites from EDC.

| Tectonic Discriminating Parameters | OIA | CIA | ACM | PM | Average Pavagada Metapelites | Average Bidaloti Metapelites | Average Bandihalli Metapelites | Duntur area Metapelite |
|---|---|---|---|---|---|---|---|---|
| Fe2O3+MgO (wt%) | 11.73 | 6.79 | 6.63 | 2.89 | 15.29 | 26.77 | 23.93 | 13.69 |
| TiO2 (wt%) | 1.06 | 0.64 | 0.46 | 0.49 | 1.00 | 1.05 | 0.75 | 1.03 |
| Al2O3/SiO2 | 0.29 | 0.20 | 0.18 | 0.10 | 0.38 | 0.23 | 0.17 | 0.39 |
| KO/Na2O | 0.39 | 0.61 | 0.99 | 1.60 | 1.14 | 1.88 | 2.11 | 1.91 |
| Al2O3/(CaO+Na2O) | 1.72 | 2.42 | 2.56 | 4.15 | 8.97 | 18.31 | 15.71 | 12.86 |

Trace elements, particularly those with relatively low mobility and low residence time in sea water such as Th, Sc, Ti, Nb and Zr are transferred quantitatively into clastic sediments during primary weathering and transportation and are thus useful tool for provenance and tectonic setting discrimination (Bhatia and Crook, 1986; McLennan, 1990; McLennan and Taylor 1991; Taylor and McLennan 1985). Bhatia and Crook (1986) have devised a scheme for distinguishing among the tectonic settings of sedimentary basins using immobile trace elements such as La, Th, Sc, Zr, Y and Co.

On the La/Sc Vs Ti/Zr (Fig. 29), Co-Th-Zr/10(Fig. 30), Sc-Th-Zr/10 (Fig. 31) and Th-La-Sc (Fig. 32) discriminating plots of Bhatia and Crook (1986) the studied metapelites plot within the oceanic island arc and continental island arc fields, confirming the Arc setting for the studied metapelites.

**Crustal evolution:**

The overall studies indicates mixing of two end member source compositions as exhibited by Pavagada and Duntur metapelites (ultramafic-mafic-intermediate) and Bidaloti & Bandihalli metapelites (mafic to intermediate). The Ni-Cr proportions indicate that the source regions of Pavagada and Duntur area had ultramafic/mafic rocks. Further the pelites also show considerable concentration of HFS elements like Th, U, Pb, Zr which could be attributed to the presence of felsic rocks of intermediate composition also in the provenance. Whereas the Bidaloti and Bandihalli pelites, indicate less mafic/ultramafic rocks and more felsic rock in the source than compared to the Pavagada and Duntur pelites. Since these pelites have low concentration of Cr, Ni and HFS elements.

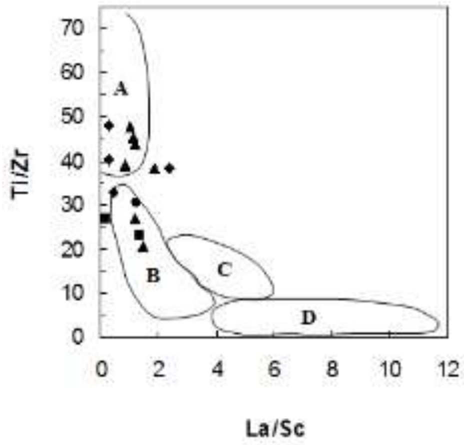

Fig. 29. La/Sc Vs Ti/Zr diagram (Bhatia and Crook, 1986), where A- Oceanic island arc; B-Continental island arc; C- Active continental margin; D-Passive margin.

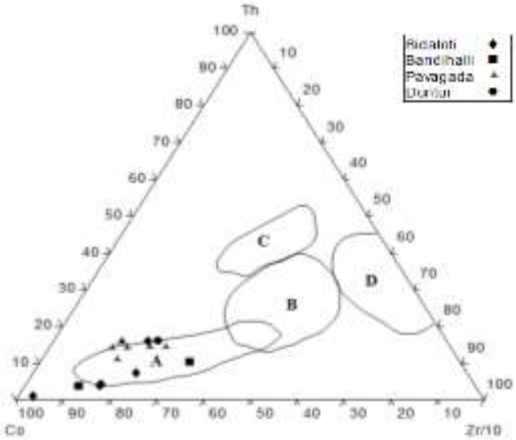

Fig. 30. Co-Th-Zr/10 ternary diagram ((Bhatia and Crook, 1986) where, A- Oceanic island arc; B-Continental island arc; C- Active continental margin; D-Passive margin.

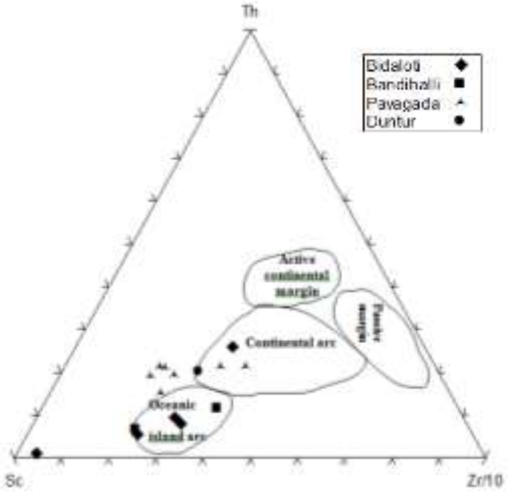

Fig. 31. Sc - Th - Zr/10 ternary diagram (Bhatia and Crook, 1986).

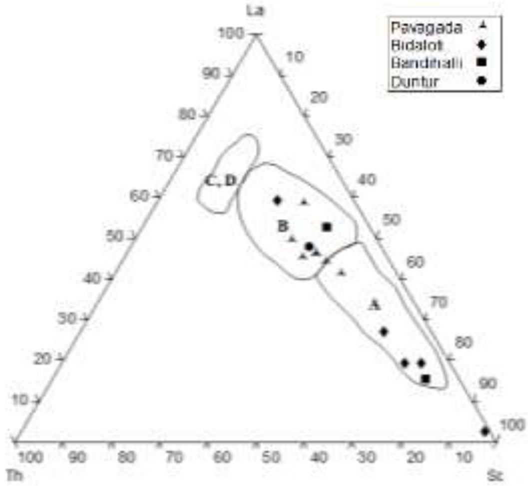

Fig. 32. Th–La–Sc ternary diagram (Bhatia and Crook, 1986) where A–Oceanic island arc; B–Continental island arc; C–Active continental margin; D – Passive margin.

The relationship among alkali and alkali earth elements, CIA and PIA values indicate that source area in the Eastern Dharwar Craton during Archaean was affected by moderate to intense weathering.

The studied metapelites defines negative εNd values at 3000 Ma with $T_{DM}$ Nd model ages ranging from 3400 to 3600 Ma (Table. V). However, the exposed archaean crust indicate ages younger than 3400Ma, which implies that their sources were derived from exotic sources localized outside the Dharwar craton (Today exposed terrains in western Australia, southern Africa or Antarctica) as all those fragments were once part of a supercontinent.

**Conclusions:**

1. Chemical characteristics of metapelites indicate their derivation from provenance comprising varying proportions of ultramafic-mafic-intermediate source.

2. The relationship among alkali and alkali earth elements, CIA and PIA values indicate that source area in the Eastern Dharwar Craton during Archaean was affected by moderate to intense weathering.

3. The studied metapelites plot within the oceanic island arc and continental island arc fields, confirming the Arc setting for the studied metapelites.

4. The studied metapelites defines negative εNd values at 3000 Ma with $T_{DM}$ Nd model ages ranging from 3400 to 3600 Ma implies that their sources were derived from exotic sources localized outside the Dharwar craton (Today exposed terrains in western Australia, southern Africa or Antarctica) as all those fragments were once part of a supercontinent.

## ACKNOWLEDGMENT

This work was fully supported by DST funded project ESS/16/272/2004 sanctioned to Prof. B. Mahabaleshwar (PI) and Dr. M. Jayananda (Co-PI), Bangalore university, Bangalore, in which I had the opportunity of working as JRF as well as SRF. I am extremely grateful to Prof. B. Mahabaleswar and Dr. M. Jayananda, for the thought provoking discussion I had with them during the course of my Ph.D. work. I thank to Dr. V. Balaram, Dr. Nirmal Charan, Dr. T. Gnaneshwar Rao and their colleagues, NGRI, Hyderabad, have extended laboratory facilities for major and trace element analysis. I am highly thankful to Dr. A.K. Choudhary and his colleagues, Geochronological division, IIT, Roorkee for providing laboratory facilities for isotopic work.

## REFERENCES

[1] Anantha Iyer, G.V. and Vasudev, V.N. (1976) Metamorphism Geochemistry, and Mineralization in Precambrian of Kolar: Geological Survey of India, Miscellaneous publications, 23 (2), pp. 596-614.

[2] Appel, P.W.U. and Mahabaleswar, B. (1988) Secular trends in rare earth elements patterns of Precambrian iron formations from India and Greenland. Jour. Geol. Soc. India., v. 32, pp. 214-226.

[3] Argast, S., Donnelly, T.W (1986) Compositions and sources of metasediments in the upper Dharwar Supergroup, South India. Journal of Geology 94, 215–231.

[4] Armstrong-Altrin JS, Verma SP (2005) Critical evaluation of six tectonic setting discrimination diagrams using geochemical data of Neogene sediments from known tectonic settings. Sedimentary Geology, Vol. 177, Issue. 1-2, Pp. 115-129.

[5] Arora, M. and Naqvi, S.M. (1993) Geochemistry of Archaean arenites formed by anoxic exogenic processes: an example from the Bababudan schist belt, India. J. Geol. Soc. India, 42: 247-268.

[6] Arora, M., Khan, R.M.K. and Naqvi, S.M. (1994) Composition of the middle and late Archaean upper continental crust as sampled from the Kaldurga conglomerate, Dhawar craton, India. Precambrian Research, v. 70, pp. 93-112.

[7] Bahlburg, H., 1998. The Geochemistry and provenance of Ordovician turbidites in the Argentine Puna. Geol. Soc. London, Special Paper 142, 127 - 142.

[8] Balaram, V and Gnaneswara Rao T (2003) Rapid determination of REE and other trace elements in geological samples by microwave acid digestion and ICP-MS. Atomic Spectroscopy, 24(6), Pp.206-212.

[9] Bavinton, O.A. and Taylor, S.R. (1980) Rare earth element abundances in Archean metasediments from Kambalda, Western Australia. Geochim. Cosmochim. Acta, 44: 639-648.

[10] Bhaskar Rao Y.J., Chetty T.R.K., Janardhan A.S. and Gopalan K. (1995) Geochronological and geothermo-barometric evidence for Neo-Proterozoic reworking of Archaean crust in the Cauvery shear zone: an Archaean-Proterozoic terrane boundary within the South Indian Granulite Province (abstract). In Precambrian '95-International conference on Tectonics and Metallogeny of Early/mid Precambrian orogenic belts, program and abstracts, pp. 209-211.

[11] Bhatia M. R. and Taylor S. R. (1981) Trace-element geochemistry and sedimentary provinces: a study from the Tasman Geosyncline, Australia. Chem. Geol. 33, 115- 125.

[12] Bhatia, M.R. (1983) Plate tectonics and geochemical cornposition of sandstones. J. Geol., v. 91, pp. 611-627.

[13] Bhatia, M.R., 1985a. Rare earth element geochemistry of Australian Paleozoic greywackes and mudrocks: provenance and tectonic control. Sed. Geol. 45. 97 - 113.

[14] Bhatia, M.R., 1985b. Composition and classification of flysch mudrocks of eastern Australia: Implications in provenance and tectonic setting interpretation. Sed. Geol. 41,249-268.

[15] Bhatia, M.R., Crook, K.A.W. (1986) Trace element characteristics of greywackes and tectonic setting discrimination of sedimentary basins. Contributions to Mineralogy and Petrology 92, 181–193.

[16] Brenner and Zander., (1996). Geoanalysis using plasma spectrochemistry - Milestones and future prospects. Analytical and Bioanalytical Chemistry 355(5-6), 559-70.

[17] Burnett, D.J., Quirk, D.G., 2001. Turbidite provenance in the lower Paleozoic Manx Group, Isle of Man: Implications for the tectonic setting of Eastern Avalonia. J. Geol. Soc. London 45, 411 - 425.

[18] Chardon, D., J.-J. Peucat, M. Jayananda, P. Choukroune, and C. M. Fanning (2002) Archean granite-greenstone tectonics at Kolar (South India): interplay of diapirism and bulk inhomogeneous contraction during magmatic juvenile accretion, Tectonics, 21, 10.1029/2001TC901032.

[19] Chardon, D., Jayananda, M., Chetty, T.R.K., Peucat, J-J (2008) Precambrian continental strain and shear zone patterns: the South Indian case. Journal of Geophysical Research-Solid Earth doi: 10.1029/2007JB005299 American Geophysical Union.

[20] Condie, K.C. and Wronkiewicz, D.J. (1990a) A new look at the Archaean-Proterozoic boundary sediments and the tectonic setting constraint. In: S.M. Naqvi (ed). Precambrian continental crust and its economic resources, Elsevier, Amsterdam., pp. 61-83.

[21] Condie, K.C., Wilks, M., Rosen, D.M. and Zlobin, V.L (1991) Geochemistry of metasediments from the Precambrian Hapschan Series, eastern Anabar Shield, Siberia. Precambrian Research, 50, 37-47.

[22] Condie, K.C., Wronkiewicz, D.J., (1990). The Cr/Th ratio in Precambrian pelites from Kaapvaal craton as an index of craton evolution. Earth Planet. Sci. Lett. 97, 256 – 267.

[23] Crook, K.A.W. (1974) Lithogenesis and geotectonic: the significance of compositional variations in flysch arenites (greywackes). In: Dott, R.H., Shaver, R.H. (Eds.), Modern and Ancient Geo-synclinal sedimentation. Society of Economic Geology, Palaeontology and Mineralogy, Special Publication, vol. 19, pp. 304–310.

[24] Cullers R L. (2000) The geochemistry of shales, siltstones and sandstones of Pennsylvanian-Permian age, Colorado, USA: Implications for provenance and metamorphic studies. Lithos, 51: 181–203.
[25] Cullers, R. L. (1988) Mineralogical and chemical changes of soil and stream sediment formed by intense weathering of the Danburg granite, Georgia, USA. Lithos 21, 301–314.
[26] Cullers, R.L., Barrent, T., Carlson, R., Robinson, B., (1987) Rare earth element and mineralogical changes in Holocene soil and stream sediment: a case study in the wet mountains, Colorado, USA. Chem. Geol. 63, 275 - 297.
[27] Devaraju, T. C. & Laajoki, K. (1986) Mineralogy and mineral chemistry of the manganese-poor and manganiferous iron- formations from the high-grade metamorphic terrain of Southern Karnataka, India. Journal of the Geological Society of India, 28, 134–164.
[28] Devaraju, T.C. and Sadashivaiah, M.S. (1969) The charnockites of Satnur and Halagur area. The Indian Mineralogist, v. 10, pp. 67-88.
[29] Eade, K.A. and Fahrig, W.F. (1971) Chemical evolutionary trends of continental plates - a preliminary study of the Canadian Shield. Geol. Surv. Can. Bull. 179, 51 pp.
[30] Eunuse Akon (1984) Petrology, mineralogy and geochemistry of the Bandite series, Karnataka. Unpublished thesis submitted to Bangalore University.
[31] Fedo, C.M., Nesbitt, H.W., Young, G.M. (1995) Unraveling the effects of potassium metasomatism in sedimentary rocks and paleosols, with implications for paleoweathering conditions and provenance. Geology 23, 921–924.
[32] Feng, R., Kerrich, R. (1990) Geochemistry of fine grained clastic sediments in the Archean Abitibi greenstone belt, Canada: implications for provenance and tectonic setting. Geochimica et Cosmochimica Acta 54, 1061–1081.
[33] Floyd P.A., Leveridge B.E., Franke W., 1991. Geochemistry and provenance of Rhenohercynian synorogenic sandstones: implications for tectonic environment discrimination: In, A.C. Morton, S.P. Todd, and P.D.W. Haughton, (eds). Developments in provenance studies. Geol. Soc. London, Special pub. 57. 173 - 188.
[34] Friend, C.R.L. and Nutman, A.P. (1992) Response of U-Pb isotopes and whole rock geochemistry to Co2 induced granulite metamorphism, Kabbaldurga, Karnataka south India. Contrib. Mineral. Petrol, 111, 299-310.
[35] Garver, J.I., Royce, P.R., Smick, T.A., 1996. Chromium and nickel in shale of the Taconic foreland: a case study for the provenance of fine-gained sediments with an ultramafic source. Journal of Sedimentary Research 66, 100-106.
[36] Gromet L. P., Dymek R. F., Haskin L. A. and Korotev R. L. (1984) The “North American Shale Composite”: Its compilation, major and trace element characteristics. Geochim. Cosmochim, Acta. 48, 2469-2482.
[37] Gu, X. X. (1994) Geochemical characteristics of the Triassic Tethys turbidites in northwestern Sichuan, China: Implications for provenance and interpretation of the tectonic setting, Geochim. Cosmochim. Acta, 58, 4615 – 4631.
[38] Gu, X.X., Liu, J.M., Zheng, M.H., Tang, J.X. and Qi, L. (2002) Provenance and Tectonic Setting of the Proterozoic Turbidites in Hunan, South China: Geochemical Evidence. Journal of Sedimentary Research; v. 72; no. 3; p. 393-407; DOI: 10.1306/081601720393.
[39] Harnois, L. (1988) The CIW index: A new chemical index of weathering: Sedimentary Geology, 55(3-4), 319-322.
[40] Harris, N.B.W. and Jayaram, S. (1982) Metamorphism of cordierite gneisses from the Bangalore region of the Indian Archean. Lithos 15, 89-98.
[41] Janardhan, A.S., Leake, B.E., Farrow, C.M. and Ravindra Kumar, G.R. (1986) The petrochemistry of the Archaean metasediments and meta-migmatites around Sargur, South Karnataka. Ind. Mineralogist, 27, 166-184.
[42] Janardhan, A.S., Shadakshara Swamy, N. and Capdevila, A.R. (1990) Trace and REE geochemistry of pelites from the Sargur high grade terrain, southern Karnataka. Jour. Geol. Soc. India, 36, 27-35.
[43] Jayananda, M. (1985) Petrological studies of high grade supracrustals and associated rocks of Bidaloti area, Tumkur district, Karnataka. Unpublished M.Phil dissertation submitted to the Bangalore University.
[44] Jayananda, M., Moyen, J.-F., Martin, H., Peucat, J.-J., Auvray, B., Mahabalesawar, B. (2000) Late Archaean (2550–2520 Ma) juvenile magmatism in the Eastern Dharwar craton, southern India: constraints from geochronology, Nd–Sr isotopes and whole rock geochemistry. Precambrian Research, 99, 225–254.
[45] Jayananda, M., Banerjee, M., Pant, N.C., Dasgupta, S., Kano, T., Mahesha, N. and Mahableswar, B. (2011) 2.62? Ga hightemperature metamorphism in the central part of the Eastern Dharwar Craton: implications for late Archaean tectonothermal history. Geological Journal. 46: doi: 10.1002/gj.1308.
[46] Jayananda, M., H. Martin, J.-J. Peucat, and B. Mahabaleswar (1995) Late Archaean crust-mantle interactions: geochemistry of LREE-enriched mantle derived magmas. Example of the Closepet batholith, Southern India, Contrib. Mineral. Petrol., 119, 314-329.
[47] Jenner G. A., Fryer B. J. and Mclennan S. M. (1981) Geochemistry of the Yellowknife Superproup. Geochim. Cosmochim. Acta 45, 1111- 1129.
[48] Kasper-Zubillaga, J.J., Carranza-Edwards, A., Rosales-Hoz, L. (1999) Petrography and geochemistry of Holocene sands in the western Gulf of Mexico: implications for provenance and tectonic setting: Journal of Sedimentary Research, 69(5), 1003-1010.
[49] Kato, Y., Kawakami, T., Kano, T., Kunugiza, K and Swamy, N. S. (1996) Rare-earth element geochemistry of banded iron formations and associated amphibolite from the Sargur belts, south India, Journal of Southeast Asian Earth Sciences, Volume 14, Issues 3-4, Pages 161-164.
[50] Kramers and Tolstikhin, (1997) Two terrestrial lead isotope paradoxes, forward transport modelling, core formation and the history of the continental crust. Chemical Geology 139(1):75-110.
[51] Krogstad, E.J,. Hanson, G.N. and Rajamani, V, (1991). U-Pb ages of zircon and sphene for two gneiss terranes adjacent to the Kolar Schist Belt, South India: evidence for separate crustal evolution histories. J. Geol. 99, 801-816.

[52] Mahabaleswar, B., Jayananda, M., Peucat, J.-J. and Shadakshara Swamy, N. (1995) Archaean high-grade gneiss complex from Satnur-Halagur-Sivasamudram areas, Karnataka, southern India: petrogenesis and crustal evolution. J. Geol. Soc. India 45, 33-49.

[53] Mahabaleswar, B., Shadakshara Swamy and Jayananda, M (1995a) Geochemistry of metapelites from archaean high grade terrains of southern Karnataka, south India. Geological Society of India, Memoir. 34, pp. 259-271.

[54] Mahabaleswar, B., Shadakshara Swamy, N and Enuse Akon (1989) Petrology of the high grade supracrustal rocks from the Bandihalli area, Karnataka. Journal of the Indian Academy of Geoscience, v. 32, pp. 140-162.

[55] Mahabaleswar, B., Vasant Kumar, I.R. and Friend, C.R.L. (1986) Geochemistry of the Archaean gneiss complex and associated rocks of the Kanakapura area, Karnataka, South India, J. Geol. Soc. India, 27, 282-297.

[56] Manikyamba, C., Balara,, V. and Naqvi, S.M. (1993) Geochemical signatures of polygenetic origin of a banded iron formation (BIF) of the Archaean Sandur greenstone belt (schist belts) Karnataka Nucleus, India. Precambrian Research, 61: 137-164.

[57] Manikyamba, C., Naqvi, S.M., and Sawkar, R.H. (1997). Identification of Sandur schist belt as a potential gold field. Curr. Sci., v.72 (7), pp.515-518.

[58] Mass and McCulloch **(**1991**)** The provenance of Archean clastic metasediments in the Narryer Gneiss Complex, Western Australia: Trace element geochemistry, Nd isotopes, and U-Pb ages for detrital zircons. Geochimica et Cosmochimica Acta, Vol. 55 (7), Pp**.** 1915-1932.

[59] Maynard, J.B., VaUoni, R. and Yu, H. (1982) Composition of modern deep sea sands from arc related basins. In: J.K. Leggett (Editor), Trench-Forearc Sedimentation. Geol. Soc. London Spec. Publ., 10: 551-561.

[60] McLennan, S.M. (1981) Trace element geochemistry of sedimentary rocks: implications for the composition and evolution of the continental crust. Unpubl. Ph.D. Thesis, Aust. National Univ., Canberra.

[61] McLennan, S.M. and Taylor, S.R. (1980a) Rare earth elements in sedimentary rocks, granites and uranium deposits of the Pine Creek Geosyncline. In: J. Ferguson and A.B. Goleby (Editors), Uranium in the Pine Creek Geosyncline. Int. Atomic Energy Agency, Vienna, pp. 175-190.

[62] McLennan, S.M., 1989. Rare earth elements in sedimentary rocks: influence of provenance and sedimentary process. Review. Mineral. 21, 169 - 200.

[63] McLennan, S.M., Fryer, B.J. and Young, G.M. (1979) Rare earth elements in Huronian (Lower Proterozoic) sedimentary rocks: composition and evolution of the post- Kenoran upper crust. Geochim. Cosmochim. Acta, 43: 375-388.

[64] McLennan, S.M., Hemming, S., McDaniel, D.K., Hansson, G.N. (1993) Geochemical approaches to sedimentation, provenance, and tectonics. Geological Society of America, Special Paper 284, 21–40.

[65] McLennan, S.M., Nance, W.B. and Taylor, S.R. (1980) Rare earth element—thorium correlations in sedimentary rocks, and the composition of the continental crust. Geochim. Cosmochim. Acta, 44: 1833-1839.

[66] McLennan, S.M., Taylor, S.R. (1991). Sedimentary rocks and crustal evolution: tectonic setting and secular trends. Journal of Geology 99, 1–21.

[67] McLennan, S.M., Taylor, S.R. and Eriksson, K. (1983) Geochemistry of Archaean shales from the Pilbara supergroups, Western Australia. Geochim. Cosmochim. Acta, 47: 1211-1222.

[68] McLennan, S.M., Taylor, S.R. and McGregor, V.R. (1984) Geochemistry of Archean metasedimentary rocks from West Greenland. Geochim. Cosmochim. Acta, 48: 1-13..

[69] McLennan, S.M., Taylor, S.R., McCulloch, M.T., Maynard, J.B. (1990) Geochemical and Nd–Sr isotopic composition of deep-sea turbidites: crustal evolution and plat tectonic associations. Geochimica et Cosmochimica Acta 56, 2015–2050.

[70] Middleton, G.V., 1960. Chemical composition of sandstones. Geol. Soc. America Bull. 71, 1011 -1026.

[71] Milodowski, A.E., and Zalasiewicz, J.A. (1991) Redistribution of rare earth elements during diagenesis of turbidite/hemipelagic mudrock sequences of Llandovery age from central Wales, in Morton, A.C., Todd, S.P., and Haughton, P.D.W., eds., Developments in Sedimentary Provenance Studies: Geological Society of America, Special Publication 57, p. 101–124.

[72] Nagender Nath, B., Kunzendorf, H., Pluger, W (2000), "Influence of provenance, weathering, and sedimentary processes on the elemental ratios of the fine – grained fraction of the bed load sediments from the Vemmbanad Lake and the adjoining continental shelf, southwest coast of India" J. Sediment. Res. 70, pp 1081–1094.

[73] Nance, W.B. and Taylor, S.R. (1976) Rare earth patterns and crustal evolution I: Australian post-Archean sedimentary rocks. Geochim. Cosmochim. Acta, 40: 1539-1551.

[74] Nance, W.B., Taylor, S.R. (1977) Rare earth element patterns and crustal evolution-II; Archaean sedimentary rocks from Kalgoorlie, Australia. Geochimica et Cosmochimica Acta 41, 225–251.

[75] Naqvi, S.M., Condie, K.C., Allen, P. (1983) Geochemistry of some unusual, early Archaean sediments from Dharwar craton, India. Precamb. Res. 22, 125–147.

[76] Nathan, S. (1976) Geochemistry of the Greenland Group (early Ordovician), New Zealand. N.Z.J. Geol. Geophys., 19: 683-706.

[77] Nesbit H. W. M., Markovics G. and Price R. C. (1980) Chemical processes affecting alkalis and alkaline earths during continental weathering, Geochim. Cosmochim. Acta. 44, 1659-1666.

[78] Nesbitt, H.W. and Young, G.M. (1989) Formation and diagenesis of weathering profiles. J. Geol., v. 97, pp. 129-147.

[79] Nesbitt, H.W., 1979. Mobility and fractionation of rare earth elements during weathering of a granodiorite. Nature 279, 206–210.

[80] Nesbitt, H.W., Markovics, G., 1997. Weathering of granodioritic crust, long-term storage of elements in weathering profiles, and petrogenesis of siliciclastic sediments. Geochim. Cosmochim. Acta 61, 1653–1670.
[81] Nesbitt, H.W., Young, G.M. (1982) Early Proterozoic climates and plate motion inferred from major element chemsitry of lutites. Nature 299, 715–717.
[82] Nesbitt, H.W., Young, G.M. (1984) Predictions of some weathering trends of plutonic and volcanic rocks based on thermodynamic and kinematic consideration. Geochim. Cosmochim. Acta 48, 1523–1534.
[83] Newton, R. C. (1990a) Fluids and shear zones in the deep crust, Tectonophysics, 182, 21-37.
[84] Nutman, A.P., Chadwick, B., Krishna Rao, B. and Vasudev, V.N. (1996) SHRIMP U/Pb zircon ages of acid volcanic rocks in the Chitradurga and Sandur groups, and granites adjacent to the Sandur Schist belt, Karnataka. J. Geol. Soc. India. 47, 153-164.
[85] Peucat, J.J., Mahabaleswar, B. and Jayananda, M. (1993) Age of younger tonalitic magmatism and granulitic metamorphism in the south India transition zone (Krishnagiri area): Comparison with older Peninsular gneisses from the Gorur-Hassan area. J. Metamorphic. Geol. 11,879-888.
[86] RAMAKRISHNAN, M. (1980) Geology of the Javanahalli, Hole Narsipur and Sargur schist belts of Karnataka craton and the geochemistry of mafic rocks. Ph.D. Thesis, Indian Institute of Science, Bangalore, 186p.
[87] Ramakrishnan, M., Viswanatha, M.N., Chayapathi, N. and Narayanan Kutty, T.R. (1978) Geology and geochemistry of anorthosites of Karnataka Craton and their tectonic significance. J. Geol. Soc. India, 19: 115-134.
[88] Roser, B. P., & Korsch, R. J. (1988) Provenance signatures of sandstone mudstone suites determined using discriminant function analysis of major element data. Chem. Geol.; Vol. 67, pp. 119–139.
[89] Roser, B.P. and Korsch, R.J. (1986) Determination of tectonic setting of sandstone-mudstone suites using SiO2, content and K2O/Na2O ratio. J. Geol., v. 94, pp. 635-650.
[90] Roser, B.P., Korsch, R.J., 1985. Plate tectonics and geochemical composition of sandstones: a discussion. J. Geol. 93, 81 - 84.
[91] Sambasiva Rao V.V., Sreenivas B., Balaram V. (1999) The nature of the Archean upper crust as revealed by the geochemistry of the Proterozoic shales of the Kaladgi basin, Karnataka, southern India. Prec. Res. V. 98. P. 53–65.
[92] Schwab, F.L. (1975) Framework mineralogy and chemical composition of continental margin-type sandstone, Geology, v. 3, p. 487-490.
[93] Schwab, F.L. (1978) Secular trends in the composition of sedimentary rock assemblages from Archaean through Phanerozoic time. Geology, V. 6, pp. 532-536.
[94] Shaw, D.M (1980) Development of the early continental crust. Part III. Depletion of incompatible elements in the mantle Precambrian Research, Volume 10, Issues 3–4, Pp. 281-299.
[95] Shaw, D.M., Reilly, G.A., Muysoon, J.R., Pattenden, G.E. and Campbell, F.E. (1967) An estimate of the chemical composition of the Canadian Precambrian shield. Can. J. Earth Sci., 4: 829-853.
[96] Taylor, S.R. and McLennan, S.M. (1981a) The rare earth element evidence in Precambrian sedimentary rocks: implications for crustal evolution. In: A. Kroner (Editor), Precambrian Plate Tectonics. Elsevier, Amsterdam, pp. 527-548.
[97] Taylor, S.R. and McLennan, S.M. (1981b) The composition and evolution of the continental crust: rare earth element evidence from sedimentary rocks. Philos. Trans. R. Soc. London, Set. A, 301: 381-399.
[98] Taylor, S.R. and McLennan, S.M. (1981c) Rare earth element evidence for the chemical composition of the Archaean crust. Spec. Publ. Geol. Soc. Aust., 7: 255-261.
[99] Taylor, S.R. and McLennan, S.M. (1985) The Continental Crust: its Composition and Evolution. Geosience texts, Blackwell Scientific Publications, Oxford. 312 p.
[100] Van de Kamp, P.C. Leake, B.E., 1985. Petrography and geochemistry of feldspathic and mafic sediments of the northeasetem Pacific margin. Trans. R. Soc. Edinb. Earth Sci. 76,411 -449.
[101] Viezer, J. (1973) Sedimentation in geological history: recycling Vs evolution or/recycling with evolution. Contrib. Mineral. Petrol., v. 38, pp. 261-278.
[102] Wildeman T. R. and Haskin L. A. (1973) Rare earths in Precambrian sediments. Geochim. Cosmochim. Acta. 37, 414-438.
[103] Wildeman, T.R. and Condie, K.C. (1973) Rare earths in Archean greywackes from Wyoming and from the Fig Tree Group, South Africa. Geochim. Cosmochim. Acta, 37: 439-453.
[104] Wronkiewicz, D.J., Condie, K.C. (1987) Geochemistry of Archaean shales from the Witwatersrand Supergroup, South Africa: source-area weathering and provenance. Geochimica et Cosmochimica Acta 51, 2401–2416.
[105] Wronkiewicz, D.J., Condie, K.C. (1989) Geochemistry and provenance of sediments from the Pongola Supergroup, South Africa: evidence for a 3.0 Ga-old continental craton. Geochimica et Cosmochimica Acta 53, 1537–1549.
[106] Young, G.M. and Nesbitt, H.W. (1999) Paleoclimatology and Provenance of the Glaciogenic Gowganda Formation (Paleoproterozoic), Ontario, Canada: A Chemostratigraphic Approach. Geological Society of America Bulletin, 111, 264-274.